Venus Atmosphere and Cloud Particle Sample Return for Astrobiology

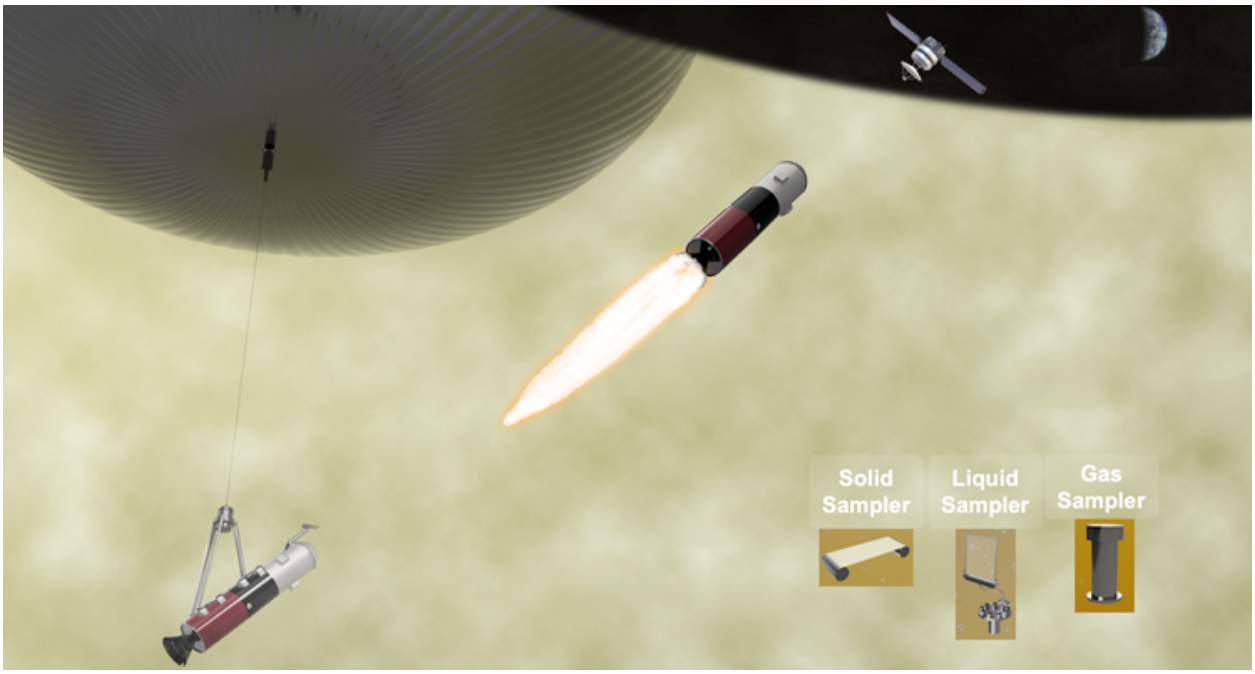

NIAC Phase I Study Final Report
January 27, 2023. Revised July 14, 2025.

TEAM MEMBERS

Principal Investigator	Sara Seager (seager@mit.edu) Massachusetts Institute of Technology
Team as listed on the NIAC proposal	Co-Investigators: Christopher E. Carr (cecarr@gatech.edu) Georgia Tech, David Grinspoon (grinspoon@psi.edu) Planetary Science Institute, Janusz Petkowski (jjpetkow@mit.edu) Massachusetts Institute of Technology Collaborators: Bethany Ehlmann (ehlmann@caltech.edu) Caltech Consultants: Kathryn Bywaters (kfbywaters@honeybeerobotics.com) Honeybee Robotics, Isabel King (irking@honeybeerobotics.com) Honeybee Robotics, Maxim de Jong (maxim@thin-red-line.com) Thin Red Line Aerospace, Sarag Saikia (saragjs@gmail.com) Spacefaring Technologies, Kris Zacny (zacny@honeybeerobotics.com) Honeybee Robotics Postdoctoral Associates: Rachana Agrawal (rachanaa@mit.edu) Massachusetts Institute of Technology, Iaroslav Iakubivskyi (iaroslav@mit.edu) Massachusetts Institute of Technology. Graduate Student: Weston Buchanan (buchanaw@purdue.edu) Purdue University

Table of Contents

Abstract

The search for signs of life beyond Earth is a motivator in modern-day planetary exploration. While our "sister" planet Venus has a surface too hot for life, scientists have speculated for decades that the much cooler atmosphere at 48-60 km above the surface might host life in Venus' clouds. A sample return of the atmosphere and cloud particles enables use of state-of-the-art instruments and facilities on Earth, greatly increasing the chances of unambiguous detection of life. We design a mission concept to return samples of the atmospheric gases, and liquid and solid particles of the cloud layers of Venus. In this study we focus on determining the feasibility of and advance the concepts of four crucial flight systems: solid sample capture; liquid sample capture, the aerial platform, and the Venus ascent vehicle (VAV). These flight systems have low Technology Readiness Level (TRL) for planetary exploration in general and pose several challenges for Venus's environment in particular. We find a feasible end-to-end mission architecture using single launch vehicle from Earth and a two-year total round-trip mission duration.

1 Introduction

For decades humans have speculated about Venus as a habitable world via its temperate cloud layer (for a review see, e.g., [1,2]). Despite unique environmental challenges of the clouds, e.g., extremely low water activity and the presence of concentrated sulfuric acid, there is an opening for the speculative idea that Venus may be inhabited by microbes in an aerial biosphere, supported by long-standing and unexplained atmospheric chemistry measurements of an unidentified strongly absorbing component and non-equilibrium gases [1,3,4]. Regardless of whether life is the answer, resolving unexplained measurements is a priority science goal for Venus studies.

Finding evidence of extraterrestrial life would be one of the most profound scientific discoveries ever made, catapulting humanity into a new epoch of cosmic awareness. We now have the ability to directly explore our nearest celestial neighbors for signs of possible life, but this search has barely begun. Venus is a compelling planet to search for signs of life because of the habitable temperatures in the cloud layers and because of many chemical anomalies [3,5,6] that together are suggestive of unknown chemistry and possibly the presence of life in Venus' clouds [5].

Indeed, the concept of life in the Venus clouds is not new; it has been around for over half a century. What is new is a realistic opportunity to envision and work toward Venus sample return.

A sample return of atmosphere and cloud particles from Venus is the optimal opportunity to explain significant atmospheric anomalies (presence of ppm of O_2, underabundance of SO_2 in the cloud layers as compared to chemical equilibrium and chemical models, the possible presence of NH_3, and more) and search for signs of life and life itself in the cloud particles. A sample return mission increases the chances of unambiguous detection of life. With a sample in hand, we can use the most sophisticated instruments on Earth, instruments with a variety and sensitivity unmatched by realistically possible spaceflight instruments, and we can follow flexible and adaptive experimental protocols not possible with a remote spacecraft investigation.

The world is poised on the brink of return to Venus with two NASA and one ESA mission planned for launch within a decade and interest from India and others. Our goal is not to supplant any other efforts but to take advantage of an opportunity for high-risk, high-reward science, which stands to possibly answer one of the greatest scientific mysteries of all, “are we alone?” and in the process pioneer the use of atmospheric sample capture in space exploration.

1.1 Sample Return Concept Description

We studied a Venus sample return mission focused on the atmosphere—intended for a sample of both the gas component and the cloud particles. The mission goal is to bring back the sample for Earth-laboratory-based study to assess the habitability of the cloud region of the atmosphere and search for signs of life or even life itself in a much more robust way than possible *in situ*. Earth laboratories have a wider variety of equipment that may reach more sensitive levels of detection as compared to in-situ space-based instruments – the same justification underpinning NASA’s $7B (FY2020) Mars Sample Return (MSR) program. We focused on pushing forward three of the least mature components of a Venus atmosphere sample return mission, leaving other components for later study:

- The atmosphere cloud particle sample capture technology (Section 4);
- The Venus ascent vehicle (VAV; Section 5);
- The aerial platform variable altitude balloon’s interface with the VAV and trade study (Section 6, 7).

In Table 1 we compare the prior state-of-the-art to our phase I goals and accomplishments, then describe our key findings in more detail.

Topic	State-of-the-Art	Eventual Goal	Phase I Goals	Phase I Accomplishments
Mission Architecture (Section 3)	Concepts for Venus sample return exist (focused on surface sampling.) A detailed end-to-end mission and systems-level concept design do not exist.	A point design with acceptable margins and reserves with an implementation approach, cost, and schedule.	Design an end-to-end sample return mission architecture and assess feasibility.	Developed an end-to-end mission architecture that demonstrates feasibility in terms of mass and power budget. CML = 2.

Solid Particle Capture (Section 4.1)	Balloons on Earth capture micrograms of microbes via sticky plates or rods with silicon oil or using filter-based material.	Up to a 10 g of bulk and single particle collection and storage by a spooled sticky tape compatible with concentrated sulfuric acid.	Prototype a sticky tape capture material and technology that can collect and store up to 1 g or up to 10^{10} individual particles down to 0.2 μm in size, that can work in a sulfuric acid environment.	Designed a spooled tape mechanism for solid particle capture on gold tape (resistant to concentrated sulfuric acid.) TRL = 3. Ready for prototyping.
Liquid Particle Capture (Section 4.2)	Commercial products exist but are too large, bulky, or power-hungry and do not capture particles with diameters < 1 μm. The expected minimum diameter for microbial type life is 0.2 μm.	Small, light-weight passive instrument with both bulk and single particle collection of relevant sizes, and compatible with concentrated sulfuric acid.	Design possibilities for small-scale, low-power active liquid particle collector based on commercial products. Prototype a small scale fog harp to determine efficiency of a passive collector. For both, work in a sulfuric acid environment.	Ruled out the need for active collectors. Built a passive fog collector prototype tested with water. Modeled sample collection for active and passive collectors for various ascent CONOPS. TRL = 2.
Venus Ascent Vehicle (VAV) (Sections 5, 7)	Mars planned sample return, but from surface, not atmosphere. Earth commercial balloon rocket launch demo in progress but without Venus' high wind speeds. Balloon gondola attitude control technology exists in balloon-borne telescopes.	An ascent vehicle of reasonable mass that can carry a 10 kg payload to Venus orbit on a precise trajectory to rendezvous with the orbiter.	Determine VAV mass to assess the feasibility of the balloon platform. Model balloon and VAV system dynamics to determine that residual motion can be controlled to accommodate a VAV launch from the atmosphere.	Determined VAV mass through trade studies of launch altitude, propellant, and stages. Modeled the dynamics of balloon and gondola system to determine the extent of the VAV pendulum-like motion. TRL =2.
Aerial Platform (Section 6, 7)	Variable altitude balloon prototype for a small payload demonstrated in Earth's atmosphere and studied for Venus, but not presently designed for carrying and launch of a small rocket.	Balloon deployment, inflation, and atmospheric sample capture with a ~2-ton payload that includes a small rocket and its launch.	Balloon requirements for VAV mass. Feasibility of variable altitude balloon for competing properties for sample collecting mobility and heavy lift/high altitude VAV delivery. Concept for aerial platform operations with other mission elements.	Determined balloon envelope mass and ballast requirements for given VAV mass and launch altitude. Developed sampling campaign and ascent CONOPS. Found a very large (~30 m) balloon is needed. TRL = 2

Table 1. Summary of proposed feasibility studies, broken down by category. TDR = technology design roadmap. TRL=Technology Readiness Level. CML=Concept Maturity Level. CONOPS = concept of operations.

Background information

Previous Venus sample return concepts mostly focused on surface sample return, with study reports as early as the mid-1980s [7–9] and continuing today [10,11]. Few focus on atmosphere only capture [11], and none to date focus on astrobiology or technical details of cloud particle capture. A detailed VAV concept, especially launch dynamics, has not been developed. Thus, our proposed mission study is unique, and most elements have not advanced beyond TRL 2 to 3. Key technologies must be developed (Table 1).

Sample return is a complex mission architecture and indeed, there are a growing number of solar system body sample returns. In addition to the planned MSR, currently ~60 g of asteroid 101955 Bennu from NASA's OSIRIS-Rex mission is on its way back to Earth [12]. NASA's Genesis mission returned solar wind samples from beyond Earth orbit in 2004 [13], and returned Stardust mission comet samples in 2006 [14,15]. Japan's JAXA mission Hayabusa retrieved micrograms of dust from the asteroid 25143 Itokawa, and Hayabusa2 recently delivered asteroid fragments from 162173 Ryugu [16,17]. The Chinese Chang'e 5 lunar sample return mission brought ~1.7 kg of lunar soil in 2020 [18]. However impressive these sample returns are, an atmosphere capture-and-return has never been attempted. This places the Venus atmosphere sample return in an entirely different category, including both instruments and the aerial platform.

1.2 Phase 1 Key Findings

We report the following key findings from our NIAC Phase I study:

1. We performed an end-to-end mission analysis and found a feasible single launch concept
    a. A feasible trajectory in 2040 has a round trip duration of 2 years with 1 year at Venus.
    b. The combined flight system mass is about 12000 kg. It can be launched on a super heavy-lift launch vehicle like Falcon Heavy Expendable, SLS, or Starship.
    c. The entry system can fit inside payload fairings with a diameter of 5 m or above.
2. We designed a spooled tape mechanism for solid particle capture on a gold tape (resistant to concentrated sulfuric acid.)
    a. The design is ready for prototyping, required to establish collection efficiency.
    b. We identified a technology gap to extract the solids from cloud droplets by evaporating sulfuric acid. To evaporate the liquid sulfuric acid, a combination of low pressure and heat is required.
3. We found that a passive aerosol harp collector is efficient and ruled out the need for power-hungry active collectors
    a. A passive collector can collect more than 30 mL of cloud droplets in an 8-day sampling campaign.
    b. The collection efficiency can potentially be increased up to 10 times with an electrostatic aerosol collector which only requires ~1 W of power.
    c. The sample amount can be scaled up with the collection area of the collector and for a longer sampling campaign duration without significant mass or power penalties.
    d. Active collectors are not appropriate in part because these use stored liquid to capture the aerosols at high efficiency which could contaminate the native sample.
    e. The passive fog collector is more efficient because it exploits the vertical winds that occur naturally on Venus.
4. We found a feasible point design for the Venus Ascent Vehicle mass and balloon system within a large trade space
    a. An 1800 kg VAV can be carried by a 27-m diameter balloon and launched from 60 km altitude to deliver a 10 kg sample canister to orbit.

b. We identified a technology gap for real-time navigation on Venus, due to Venus' lack of a magnetic field and due to the optically dense cloud deck a lack of visuals (sun, stars, terrain) during the VAV launch and initial ascent phases.

5. We found a feasible balloon design to carry the 2-ton gondola
    a. A single envelope variable altitude balloon of 27-m diameter can carry a 2-ton gondola for a sustained duration of more than 1 week during which time the balloon platform would drop ballast for a controlled ascent.
    b. The balloon carries additional ballast as a contingency feature to tackle unintentional helium leaks.
    c. High inflation rates are required for the balloon envelope given its large volume and short descent time. An inflation rate as high as 40 times that of Vega balloons is required. (Vega's balloon volume was 15 m^3 and inflated in 4 minutes; ours has a balloon volume of over 7000 m^3 to be inflated in 30 minutes).
    d. The balloon envelope's limits in terms of the inflation rates and dynamic pressures it can sustain are major design drivers for sizing the parachute system.
6. We analyzed the dynamics of the balloon-gondola system
    a. The gondola spin rate response is less than 1 deg/s for the expected wind gusts at Venus. These rates can be controlled using existing technology used to control the pointing of balloon-borne telescopes.

2 Science Concept of Operations

Goal Determine altitudes of interest for sample capture as an input requirement for balloon operation.

Background The driving science goal is to collect up to 10s of grams of samples from Venus atmosphere, including gas, liquid, and solid. The total sample mass is yet to be determined, and will depend on collection capabilities, storage, and transfer. The present mission design has a 10 kg sample canister of which 500 g is allocated to the return sample.

Method We qualitatively investigated balloon operation scenarios (Figure 1) while considering altitudes of interest.

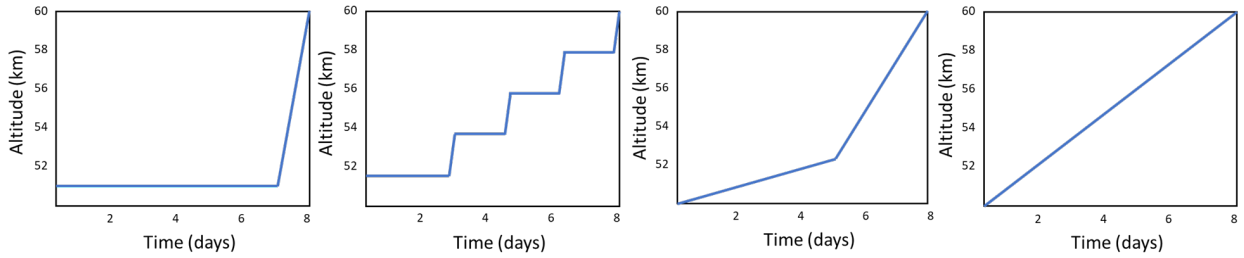

Figure 1. Ascent and sampling paths. The x-axis shows the time spent in the atmosphere in days. The y-axis shows altitude above the Venus surface in km. We consider four sampling paths, each with different balloon and sample collection capabilities.

Key Findings Sample return from 48 to 60 km is of interest, with emphasis on the lower cloud altitudes where the large and reportedly inhomogeneous cloud particles are [19,20]. We realized that a constant ascent rather than cycling between altitudes is adequate, as long as enough time is spent at a given altitude. We considered four options, as shown in Figure 1, using our sample collection model (Section 4.2) to inform duration at each altitude. We chose the third option with about four days at lower cloud altitudes (from 48 to 52 km) and about four days ascending from 52

to 60 km (i.e., middle and part of upper clouds). The ascent path is a key input to the balloon design and sampling strategy.

3 Baseline Mission Concept

> ***Novel Result:*** *Most of the previous Venus sample return concept studies focused on surface sample return and none on astrobiology. We designed an end-to-end mission concept for atmosphere sample return and determined initial feasibility by quantifying key performance parameters (sampling rate, VAV, and balloon mass), and performing basic mass and power budget analyses.*

Goal To design and analyze an end-to-end mission architecture for cloud sample return from Venus

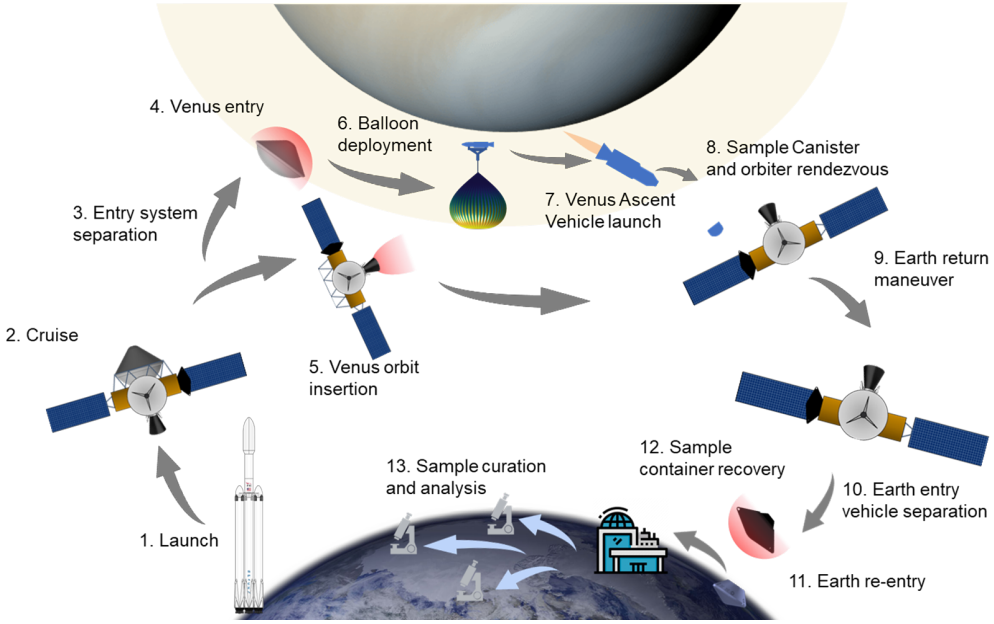

Figure 2. Schematic of the mission architecture for the Venus atmosphere sample return. After launch and cruise, the flight system separates into two components, the entry probe and the orbiter. The entry probe consists of a variable-altitude balloon operating between 48-60 km altitude above the surface. The balloon's gondola contains the sample capture hardware, as well as the Venus ascent vehicle. The aerial platform spends a week capturing samples while rising from 48 to 60 km altitude, after which the Venus Ascent Vehicle will launch and rendezvous with the orbiter. The orbiter serves as the return vehicle to Earth, and delivers the sample to Earth for recovery.

and determine mission feasibility.

In this Section, we describe the baseline mission concept that we came up with as a result of the Phase I effort, based on various trades studies. The baseline mission returns up to 500 grams of atmosphere sample (gas, liquid, solid) to Earth. The details of the subsystems, trade studies, and technologies are given in subsequent Sections.

3.1 Mission Architecture

The Venus Atmospheric Sample Return spacecraft consists of two main elements, the entry system and the orbiter. The entry system consists of the aerial platform that will collect the sample and also carry the Venus Ascent Vehicle (VAV) that will transfer the sample to Venus orbit. The orbiter will capture the sample delivered to Venus orbit by the VAV and return to Earth. The orbiter will also function as a communication relay during the mission of the aerial platform. The sample is returned in a canister that is transferred to Earth in the Earth Entry Vehicle and recovered on the ground or ocean. The sample is then curated at a facility on Earth and distributed to labs around the globe. See Figure 2.

3.2 Key Mission Trades

To meet the goals of our Phase I study, we performed several key trades throughout the study:

1. Earth-Venus trajectory analysis for options that are energy efficient but also allow a short round-trip mission duration.
2. The liquid capture mechanism options, to compare the active vs passive methods for mass, power, and collection efficiency.
3. Variable altitude balloon types to select a simple and mass-efficient design that can carry over 2-ton payload and control ascent.
4. VAV sizing trades that include optimal launch altitude selection, propulsion type, and number of stages.

Table 2 shows the various options for each of the trades and the green highlighted cells represent the selected baseline options. We provide the details of each of the trade studies in subsequent Sections of the report. We also performed other qualitative trade studies that are not shown in the table but are mentioned throughout the report.

		Option 1	**Option 2**	**Option 3**	**Option 4**
Trajectory		Short stay	Long stay	Low-thrust	
Liquid Capture		Active Cyclone	Passive fog harp	Electrostatic fog harp	
Balloon	Variable altitude balloon design	Single envelope ballast control	“Light-bulb”	Mechanical Compression	
	Balloon ascent CONOPS	Collect at ~51 km and rise to launch	Hold at various altitudes	Variable climb rate, no hold	Constant climb rate, no hold
VAV	VAV launch altitude	60-63 km	64-67 km	68-70 km	
	VAV propulsion	Solid	Hybrid	Liquid	
	VAV stages	Single	Two-stage		

Table 2. Summary of key trade studies with the corresponding options considered. The green highlighted options are chosen for the baseline point design.

3.3 Mission Operations

In this Section we describe the details of each of the following broad mission phases and the concept of operations: (1) Launch from Earth and the interplanetary trajectory; (2) Entry, Descent, and Inflation on Venus; (3) Balloon ascent and the sampling campaign; (4) VAV launch preparation and launch; (5) Orbital rendezvous and Earth return.

3.3.1 Launch and Round-trip Interplanetary Trajectory

Goal Select a baseline round-trip trajectory between Earth and Venus to evaluate the overall mass budget and launch feasibility of the spacecraft.

Method We used Lambert arc solutions to generate trajectory options from 2035 to 2043. The inertial position of Venus with respect to Earth repeats approximately every 8 years. Therefore, a baseline trajectory in this period can be repeated every 8 years. The objectives of trajectory selection are to maximize the launch mass margin (given entry system and orbiter dry mass) and minimize round-trip mission duration.

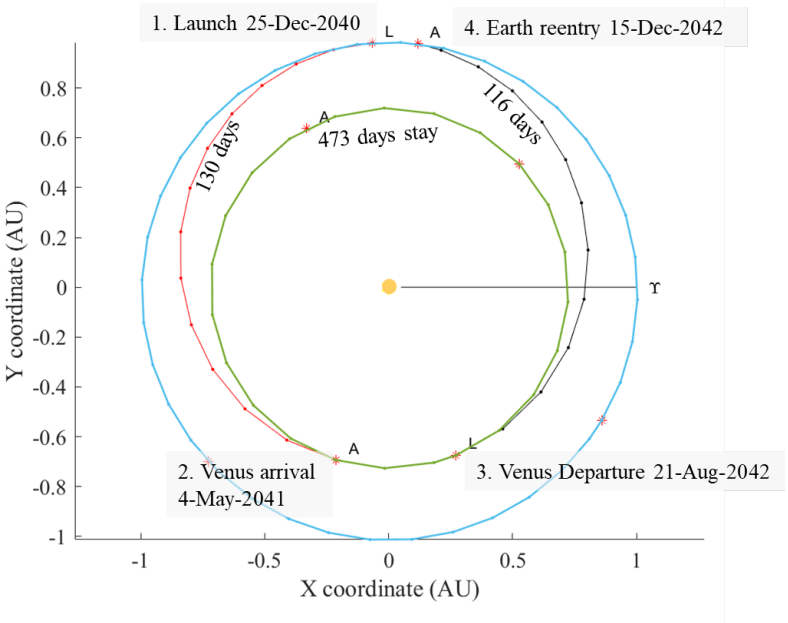

Figure 3. The baseline round-trip interplanetary trajectory from Earth to Venus. The x and y axis are the coordinates in the sun-centered inertial frame in astronomical units (AU).

Key Results We evaluated a 2040–2042 round-trip trajectory for the mission with a total mission duration of just over 2 years. See Figure 3. We chose a launch option on a ballistic Trans Venus Trajectory in December 2040 with a launch C_3 of 7.2 km^2/s^2. It takes about 130 days to reach Venus. The stay time in Venus orbit would be about 15 months (including a week-long sampling campaign in the Venus cloud layers), after which the Earth Return Vehicle would begin the return journey on a ballistic trajectory. The Earth Entry Vehicle carrying the Sample Return Canister (SRC) would enter Earth's atmosphere in December 2042. The mass margin for a launch on the SLS Block 1 is about 70% and for launch on the Falcon Heavy Expendable is about 6%. We propose to iterate the mass estimates and incorporate systems margins in Phase II.

3.3.2 Entry, Descent, and Inflation

Goal Model and evaluate the entry, descent, and inflation (EDI) of the aeroshell through the Venus atmosphere, in order to size the entry system and parachute system.

Method We modeled the atmospheric entry dynamics of the entry system using the following parameters: (1) Entry velocity = 10.6 km/s; (2) Entry flight path angle = -8 deg; (3) Entry interface altitude = 180 km; (4) Ballistic coefficient = 223 kg/m^3. We simulated the entry dynamics for a range of entry angles and aeroshell diameters and found the above parameters satisfy the constraints.

The parachute system is sized to satisfy two constraints: (1) descent time should be greater than 30 minutes and (2) dynamic pressure during balloon inflation should be less than 20 Pa.

Key Results Figure 4 shows the EDI concept of operations (CONOPS) and trajectory.

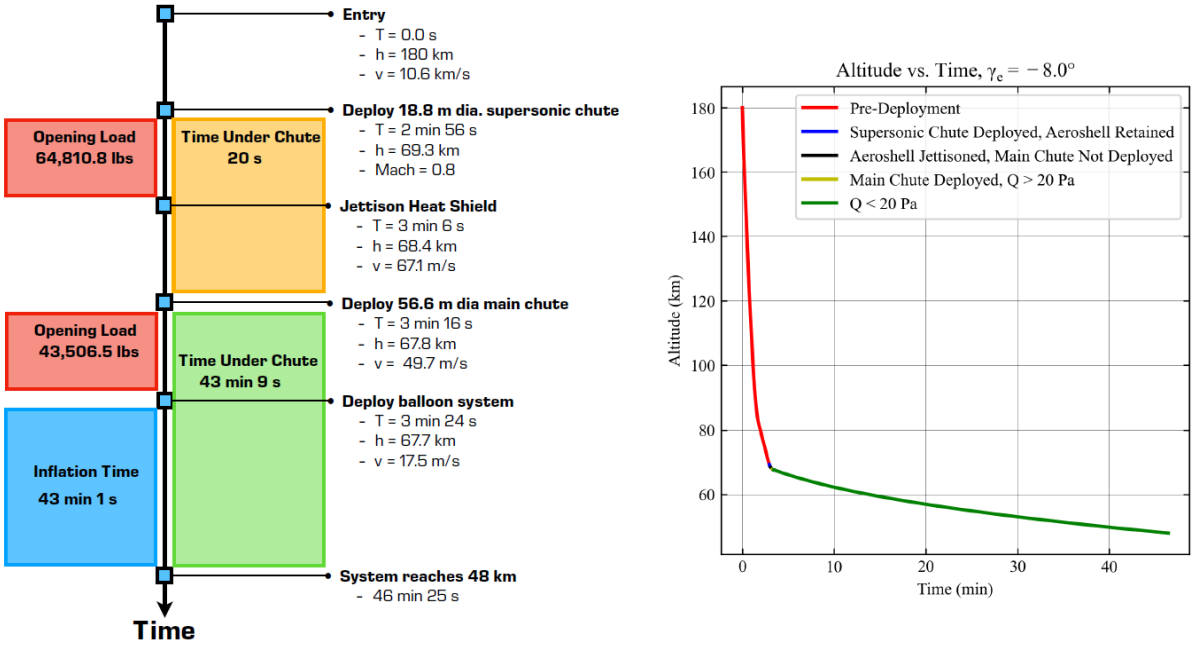

Figure 4. Concept of operations of the entry, descent, and inflation (EDI) events. (Left) A timeline of the critical events from entry, followed by deployment of the supersonic parachute at Mach 0.8 and heat shield jettison, followed by main parachute deployment and balloon inflation for 43 minutes. (Right) EDI trajectory plot with time on x-axis and altitude on y-axis.

We found that the parachute system design is driven by the dynamic pressure constraint of 20 Pa. To satisfy this constraint, a 56.6 m diameter main parachute is required. For the given entry conditions, a descent time of 43 minutes would be achieved. The opening load for a single parachute system is extremely high, about 400,000 lbs, which is greater than the largest load ever survived by a supersonic parachute as of late 2018 (Mars 2020 parachute records 67000 lbs). So, we added a supersonic parachute of 18.8 m diameter that reduced the opening load on the main parachute to ~43,000 lbs.

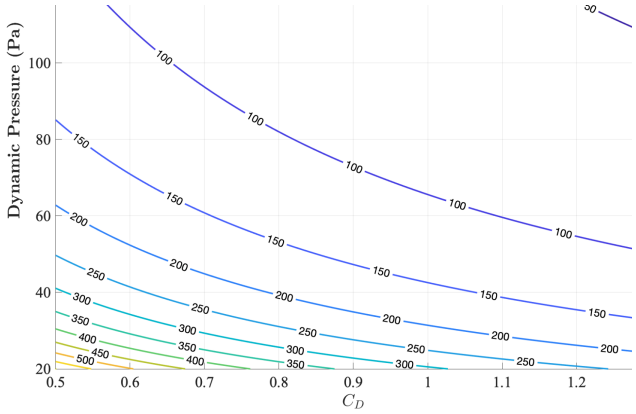

Figure 5. Contour plots of (Top) parachute diameter (m) and (Bottom) mass (kg) as a function of dynamic pressure constraint (y-axis) and the drag coefficient of the parachute (x-axis).

One of the key findings was the influence of the dynamic pressure constraint during inflation. This constraint was obtained from the balloon envelope's load limits during inflation. We found that increasing the load limits of the balloon had a significant impact on the parachute mass and the overall mass of the spacecraft. Figure 5 shows the diameter and mass of the main parachute as a

function of the dynamic pressure constraint and the drag coefficient. The mass of the parachute decreases two times for an increase in dynamic pressure from 20 Pa to 40 Pa, reducing the entry system mass by almost 10%. One of the tasks in Phase II is to test the balloon inflation under dynamic loads and revise the constraint.

3.3.3 Balloon Ascent and Sample Collection CONOPS

Goal Select the altitude range for balloon operations and design a baseline concept of operation of the balloon and gondola systems.

Background Information The samples should be collected from 48–60 km (Section 2). The maximum altitude required for the balloon to ascend to is the launch altitude of the VAV, which is, therefore, at or above 60 km (Section 5).

Method We considered four options for the balloon ascent CONOPS (see Section 2). We narrowed down to two options: (1) constant ascent rate and (2) variable ascent rate with more time spent in the lower cloud layer. We compared the sampling campaign for the two CONOPS using our sample flow and collection model (see Section 4.2.1) to choose the baseline CONOPS.

Key Results The balloon has a net upward lift that allows it to ascend at a predetermined rate. The ascent rate can be increased by dropping ballasts. The baseline sampling campaign duration is eight days, during which the balloon would ascend and collects samples from 48 km to 60 km altitude, allowing sampling from the lower, middle, and part of the upper cloud layers. The balloon would cover a range of 48–52 km in the first four days. In the next four days, the balloon would ascend faster to cover the altitude region from 52 km up to 60 km. In order to comply with the scientific objectives, the platform will spend half of the sampling time in the lower clouds (48–52 km). Figure 6 shows a notional concept of operations of the various subsystems during a 24-hour period. This CONOPS is approximately repeated every 24 hours. This CONOPS is just an example and is proposed to be revised in Phase II.

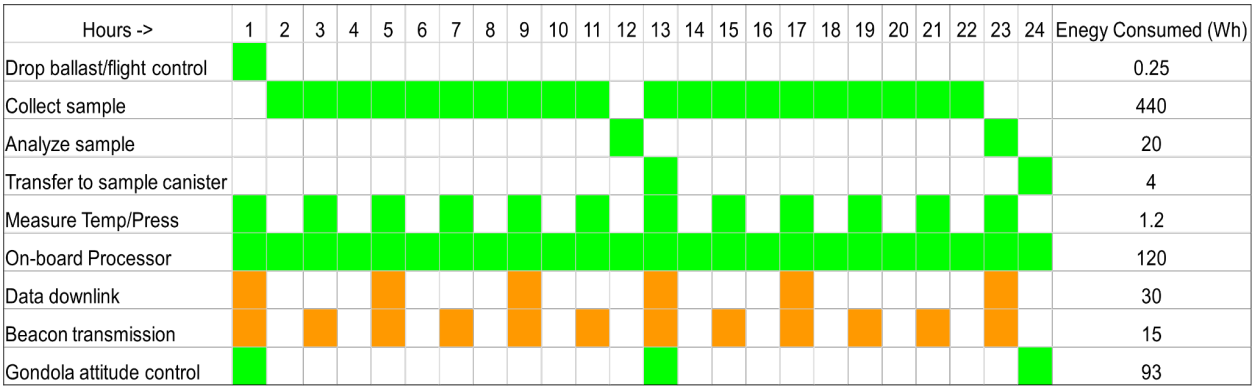

Figure 6. A notional CONOPS of the gondola subsystems during the sampling campaign. The orange color for communications means it is dependent on the orbiter pass time and duration.

The total energy consumed every 24 hours would be about 725 Wh. For the 8-day mission, primary batteries would be mass-efficient (i.e., the high energy density at low mass) and simpler than deploying solar panels. But increasing the mission duration is an attractive trade to allow more samples to be collected. The super-pressure balloon can maintain buoyancy for over a month due to the low-permeability envelope material. For such a long mission, solar panels would be more mass-efficient than primary batteries (e.g., quadruple junction solar cells).

3.3.4 VAV Launch Preparation and Launch Trajectory

Goal Determine the optimal launch altitude and launch trajectory of the VAV. Design baseline CONOPS for launch preparation to identify the systems involved.

Background info The VAV launch altitude is a crucial mission parameter. Since the Venus atmosphere is significantly dense even at higher altitudes (0.3 bar at 60 km), the higher the launch altitude the smaller the drag force on the VAV. But the balloon size and mass would also increase for higher altitudes, leading to competing system mass parameters.

The balloon's location during the launch is not precisely chosen but should fall within two main constraints. One is the launch location should be close to the equator, as opposed to higher latitudes to avoid higher meridional winds. Second, the launch location should not be above highlands such as Aphrodite Terra to avoid gravity waves (upward wind motion due to highlands).

Method We performed optimization of the VAV launch trajectory using the GPOPS-II software for given input of number of stages, propellant type, and launch altitude. The objective of optimization is to maximize the final mass in orbit and the control variable is the pitch angle of the rocket. See Section 5 for details on launch altitude selection and launch trajectory optimization.

Key Results After the sample collection operation across the altitude range of 48 to 60 km, the balloon ascent gradually slows down to halt at 60 km. The Sample Return Canister (SRC) would be sealed and transferred to the VAV using a robotic arm. The VAV payload adapter is closed for launch. The VAV systems are checked for launch readiness. The gondola attitude determination and control system is engaged in maintaining the launch azimuth of the VAV.

Once all the systems are ready, the VAV is released from the gondola and the first stage solid rocket motor is ignited. The first stage burns for about 45 seconds. The rocket then coasts for about 150 seconds, after which the first stage is jettisoned. The second stage solid rocket is ignited and burned for about 25 seconds to insert the payload into a 180 km by 300 km orbit. The second stage is released after the insertion. The remaining systems are in orbit until they reach 300 km altitude, where the RCS is used for a final orbit-trim maneuver to inject the SRC in a 300 km circular orbit. See Figure 7.

3.3.5 Orbital Rendezvous and Return

We describe a high-level and notional sequence of events for orbital rendezvous at Venus and the return of the samples to Earth. Once the SRC is injected into the orbit, the orbiter performs rendezvous maneuvers to capture the SRC. The orbiter will use the SRC’s beacon and optical inputs to localize the position of the SRC. The viability of using an optical method for rendezvous needs to be studied further for Venus because of its high albedo.

Once the SRC is captured, the orbiter raises its orbit to avoid orbital decay due to drag. The orbiter remains in the raised orbit till the opportunity to return to Earth opens up, about 15 months from arrival. The Earth Return Vehicle then performs a chemical burn to return to Earth. Upon arrival at Earth, the Earth Entry Vehicle is released. Then it performs hypersonic entry, descent, and landing to deliver the SRC to the recovery site.

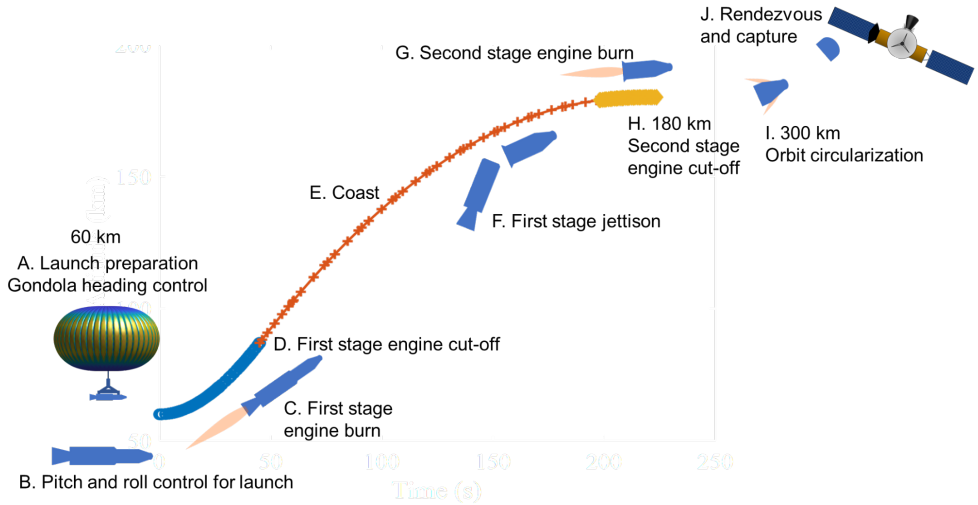

Figure 7. Schematic of the VAV launch CONOPS. The balloon halts ascent at 60 km, where the VAV heading is adjusted. The VAV is dropped from the gondola and the first stage is ignited. After the first engine cut-off, the VAV coasts for about 2.5 minutes before jettisoning the first stage. The second stage is ignited and VAV injects into a 180 km by 300 km altitude. At 300 km, a circularization burn is performed followed by rendezvous with the orbiter.

3.4 Flight Systems

Goal Size the critical flight systems to obtain overall mass and power budget and determine launch feasibility.

Method We divided the spacecraft into main systems and subsystems and estimated the mass of the individual subsystems. The systems-level breakdown of the spacecraft is shown in Figure 8. We describe the baseline design and sizing method of the main flight systems in the subsequent subsections: Balloon, Venus Ascent Vehicle, Gondola, Entry System, and Orbiter.

System	Mass (kg)
Total Spacecraft Launch Mass	12381
Entry System	6598
Orbiter Wet Mass	5783
Orbiter Dry Mass	815

Table 3. Mass budget summary of the Venus Atmospheric Sample Return spacecraft.

Key Results The mass and power budget of the entry probe is shown in Table 3.

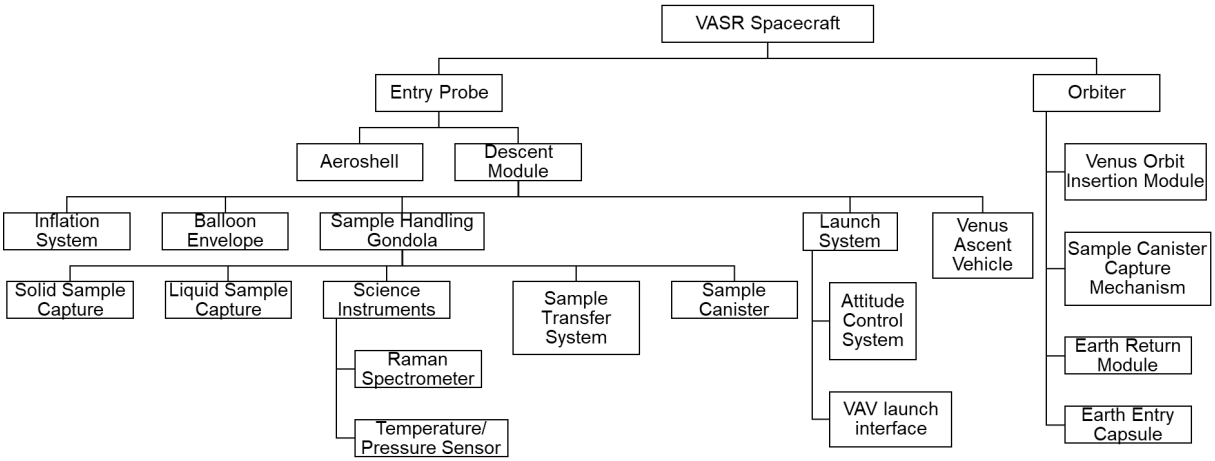

Figure 8. Spacecraft systems level schematic. (VAV = Venus Ascent Vehicle).

3.4.1 Balloon

Goal Determine a feasible mass and size for the balloon for given VAV launch altitude and gondola mass.

Method We considered three design options for the variable altitude balloon: (1) single envelope using ballast-drop and gas-venting control; (2) motorized altitude variation using either mechanical compression or pumped helium; (3) a “light bulb” design that is a hybrid of single envelope and mechanical compression design. Further description of these designs and our rationale for selecting the single envelope design is given in Section 6.

Key Results The aerial platform is a single envelope Ultra-High Performance Vessel (UHPV) (Section 6.1, Figure 30). The balloon uses a combination of precision ballast drop and lifting gas venting. The balloon diameter is ~27 m when fully expanded at the maximum altitude of 60 km.

Parameter	Value	Unit
VFA Balloon volume @ maximum altitude	7,270	m^3
VFA Balloon diameter	27.22	m
VFA Balloon height	16.33	m
IN-FLIGHT SYSTEM TOTAL		
VFA Balloon Envelope mass	377	kg
Free lift (7.5%)	230	kg
VFA Balloon Ballast and/or reserve gas (15%)	460	kg
Gondola total allowable mass	2001	kg
Gondola mass fraction of In-Flight System	65.2	%
VFA Balloon packaged volume (ROM)	9.2	m^3

VFA in-flight system total mass	3068	kg
INFLATION SYSTEM (JETTISONED)		
Tank mass	240.7	kg
Helium mass	18.1	kg
Regulator, valve, plumbing mass	9.1	kg
Inflation System total mass	267.9	kg

Table 4. Mass breakdown of the aerial platform, including inflation system mass. (VFA = Variable Float Altitude).

3.4.2 Venus Ascent Vehicle

Goal Determine a mass and size for the VAV as well as a qualitative design and operational scenario in concurrence with the balloon platform design.

Method We selected the baseline configuration of VAV from a range of options on the propellant type and the number of stages. The criteria for selection were to minimize total mass and risk. The mass of the VAV also depends on the launch altitude and required performance (injection orbit and payload mass). Launch altitude is a critical trade study that also involves balloon sizing Refer to Section 5 for details on the trade studies and design.

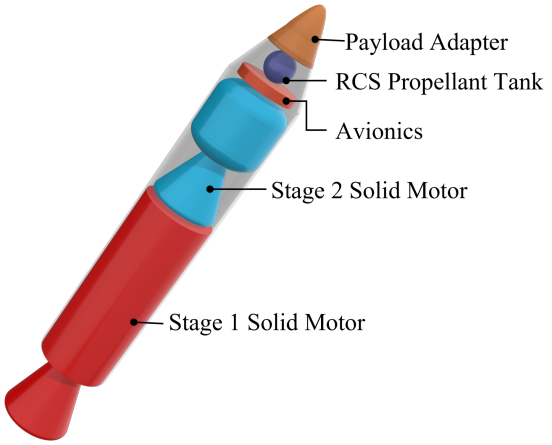

Figure 9. Notional schematic of the Venus Ascent Vehicle indicating major subsystems.

Key Results The Venus Ascent Vehicle (VAV) is a 2-stage solid rocket that delivers a 10 kg Sample Canister to a 300 km Low Venus Orbit. The VAV uses electro-mechanical thrust vector control for pitch and yaw control. It has a Reaction Control System (RCS) for spin control, attitude control during the coast and second stage burn, and orbit insertion in the final stage. The structure is coated to protect against sulfuric acid. The first stage and RCS nozzles have covers to protect from sulfuric acid and debris during the atmosphere sampling campaign. The VAV Gross Lift-Off Mass (GLOM) is 1840 kg. The VAV is 4.7 m long and 0.8 m in diameter. Figure 9 shows a schematic of the VAV.

3.4.3 Gondola

Goal Perform rough order of magnitude mass estimate of the aerial platform gondola subsystems.

Method We refer to all the systems in the aerial platform other than the balloon envelope as the gondola. The gondola consists of three main systems: Sample Management System, Launch System, and the Venus Ascent Vehicle. Figure 10 shows a schematic of the gondola. We perform detailed sizing of some of the sample capture systems and the VAV. Other systems are sized based on analogies from commercial or planetary technology. For example, we derive the sample canister design from the MSR Orbiting Sample (OS) container. The Sample Transfer Arm is based on the Mars Surveyor 2001 Robotic Arm with an 80 N end effector load capacity. We double the mass and power estimate of the arm to be able to lift the 10 kg sample canister against Venus's gravity.

Key Results The subsystems of the gondola are described below. Table 5 provides the mass breakdown of the subsystems.

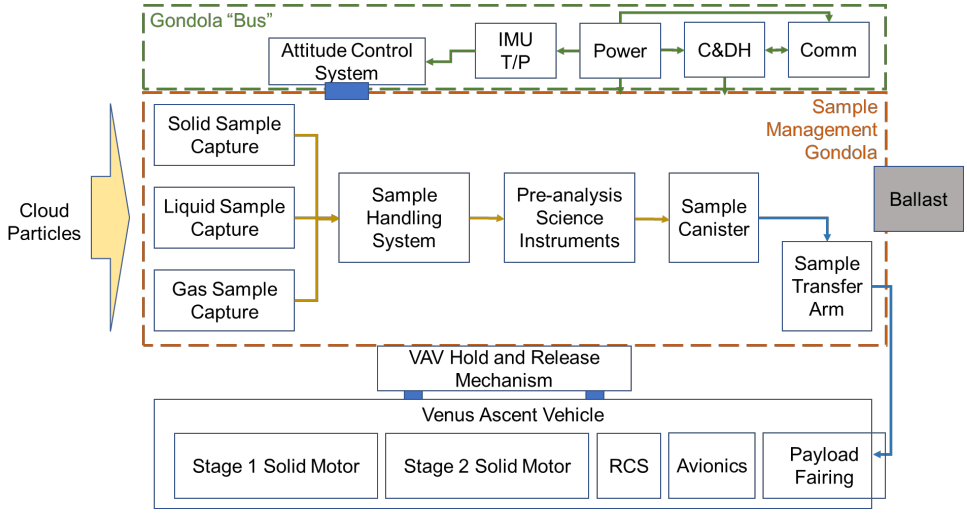

Figure 10. Block diagram of the gondola subsystems.

The *Solid Sample Capture (SSC)* system is a flexible spooled tape mechanism to capture aerosol particles on a gold tape (resistant to concentrated sulfuric acid).

The *Liquid Sample Capture (LSC)* system is a passive aerosol harp using a metal wire mesh to collect sulfuric acid droplets.

The notional *Sampling Handling System (SHS)* consists of a carousel of sample tubes that are sealed and transferred to the sample canister.

The *Sample Return Canister (SRC)* weighs 10 kg and is sized to return up to 500 grams of sample to Earth. It uses passive thermal control to maintain the temperature of the sample within its native environment temperature range. Once the SRC rendezvous with the orbiter, the Earth Entry Vehicle will provide additional thermal protection.

Systems	Mass (kg)	Power (W)	Duration of Operation (hr)	Energy Usage (Whr)
Sample Management Gondola	130			6878
Solid Sample Capture	4.1	20	144	2880

	Liquid Sample Capture	5	2	144	288
	Sample Handling System	5	2	5	10
	Science Instruments				
	Raman Spectrometer	15	10	16	160
	Temp/Press Sensor	0.5	0.1	192	19.2
	Sample Transfer Arm	10	84	1	84
	Sample Canister	10	0.1	1	0.1
	Communication	5	20	112	2240
	C&DH	5	5	192	960
	Power	20	1	192	192
	Structure and Thermal	30			
Launch System		132			
	Attitude Control System (CMG)	61	31	1	31
	VAV hold and release mechanism	35			
	Frame Structure	36			
Venus Ascent Vehicle		1840			

Table 5. Mass breakdown of the gondola components.

3.4.4 Entry System

Goal Determine the mass and volume of the entry system components and qualitatively determine launch feasibility.

Method The entry system was sized to accommodate the VAV, stowed balloon envelope, inflation system, and the gondola. The diameter of the entry system is constrained by the length of the VAV, which is 4.7 m. We considered a baseline diameter of 5 m to be sufficient. Since the fairing of a Falcon Heavy or SLS is equal to or greater than 5 m, we chose a rigid aeroshell design for the entry system. We choose a bi-conic 60-degree sphere cone aeroshell design due to high packaging and aerothermodynamic efficiency. The resulting ballistic coefficient of the entry system is 223 kg/m^2 (given mass and area, and Cd of ~1.5), which is higher than the Pioneer Venus probes (180 kg/m^2). But we selected a trajectory with a slower entry speed of 10.6 km/s and entry flight path angle of -8 deg (compared to 11.5 km/s and -25 deg for Pioneer Venus probes), leading to lower g-loads and heat rate albeit higher total heat load. We assumed a mass fraction of over 40% for the aeroshell system including heat shield, structure, and backshell, which is similar to the Pioneer Venus probes mass fraction.

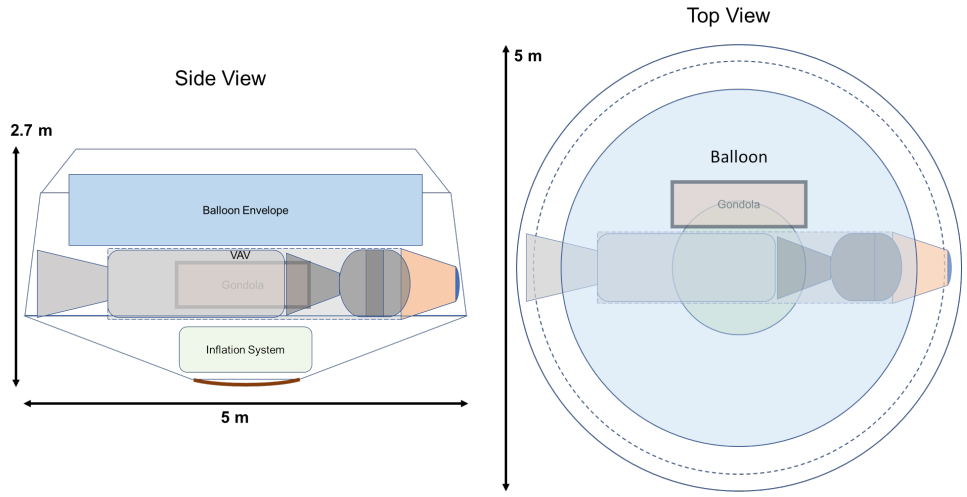

Figure 11. Schematic of the entry system showing the system accommodation.

Key Results Figure 11 shows the schematic of the entry system with the descent systems inside. There is room for more efficient accommodation of the systems and reducing the backshell size. Table 6 shows the mass breakdown of the entry system.

There is further scope for mass reduction, especially for the parachute system. This analysis is a proposed Phase II task, as we further study the parachute system requirements during inflation. We will also keep the trade between a rigid aeroshell, ADEPT, and inflatable entry system open as further mass benefits can be obtained from these advanced technologies.

Systems			**Mass (kg)**
Entry System			6589
	Aeroshell		2471
	Descent Module		4118
		Parachute and Mortar System	675
		Inflation System	270
		Balloon Envelope	377
		Free Lift Ballast	260
		Ballast and reserve gas	460
		Sample Management Gondola	125
		Launch System	132
		Venus Ascent Vehicle	1840

Table 6. Mass breakdown of the entry system component.

3.4.5 Orbiter

Goal Estimate the mass of the orbiter.

Key Results We did a rough order of magnitude mass estimate of the orbiter. Table 7 provides the mass breakdown. The Earth Entry Capsule mass is based on the OSIRIS-Rex return capsule. The propulsion systems are separated for Venus Orbit Insertion and Venus departure maneuver to and from the 300 km orbit and assume a roughly 8% tank factor. A 200 m/s ΔV is allocated for the orbital rendezvous maneuver with the Venus departure propulsion system.

Systems			Mass (kg)
Orbiter Wet Mass			5783
Orbiter Dry Mass			815
	Spacecraft Bus		295
		Structure and Mechanisms	100
		Thermal Control	25
		Power	86
		TT&C	29
		C&DH	17
		ADCS	25
		Other	13
	Sample Canister Capture Mechanism		60
	Earth Return Module Dry Mass		90
	Earth Entry Capsule		50
	Venus Orbit Insertion Module Dry Mass		320
Venus Orbit Insertion Propellant			3928
Venus Departure Burn Propellant			1043

Table 7. Mass breakdown of the orbiter.

4 Sample Collection

Novel Result: *Aerial liquid and solid sample collection needs a pioneering approach as it is yet to be attempted on another planet. We found a solution for efficiently capturing liquid droplets from an aerial platform—a modified fog collector—and built a prototype while ruling out the need for power-hungry active collectors. For solid sample capture, we created a design of a flexible tape and roller sampling system which is inherently small and flexible and allows modular integration with instruments if desired.*

Sample collection from a planetary atmosphere is a new field of engineering research. We aim to collecting sample in all of Venus' cloud layers. The nature of particles is not entirely known. While

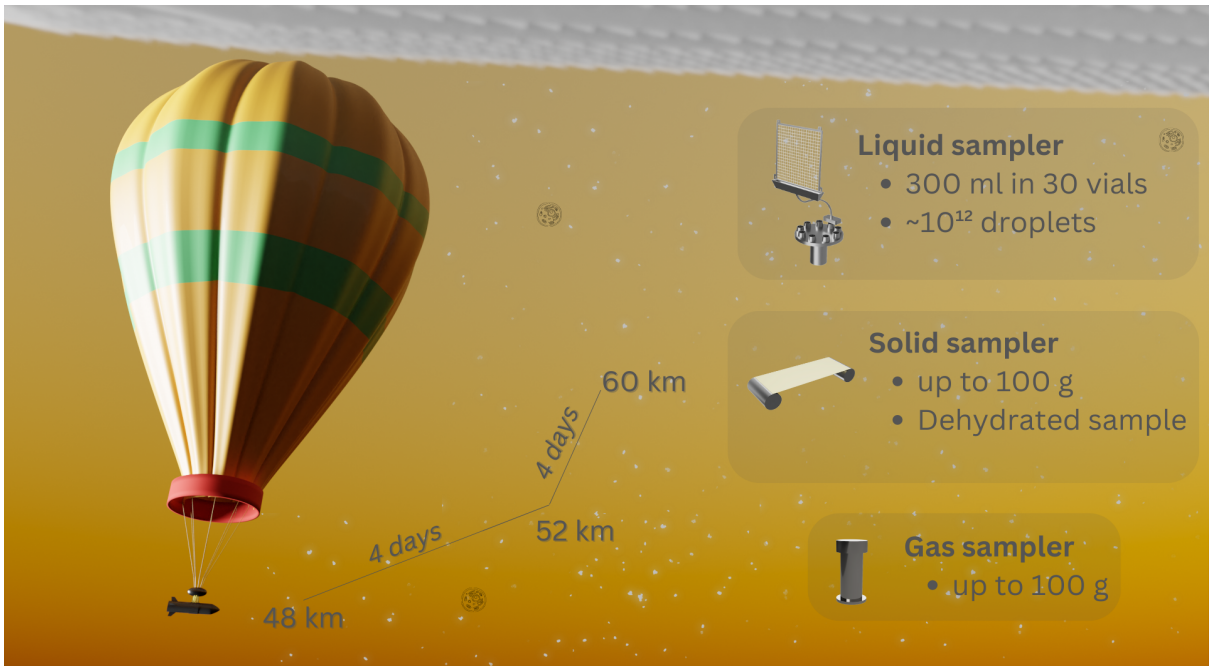

Figure 12. The aerial platform ascent and sampling CONOPS. The balloon and VAV are to scale. The sample mass indicated for the liquid, solid, and gas sample are maximum example collected amounts, with actual values proposed for a Phase II study.

the primary assumption points out that clouds are made from liquid spherical particles, the Pioneer Venus Particle Size Spectrometer showed evidence of non-spherical ~7-µm-large particles in the lower cloud layer [19]. One explanation for the non-spherical particles is the presence of solid material. Therefore, the platform will host three types of samplers: liquid, solid, and gas. In this study, we evaluated and made a preliminary design assessment for the liquid and solid collectors; the gas collector is out of scope for this report and would be addressed during a later study phase.

4.1 Solid Sample Collector

Goal Develop a prototype instrument design for capturing aerosol solid samples from the cloud particles using a spooled tape mechanism.

Background information The Honeybee Robotics team (henceforth, HBR) previously developed the concept for an all-in-one collection, delivery and sealing mechanism for in situ analysis of solid particles in the Venusian atmosphere [21]. The concept utilizes a tape wound between two spools: the feed and storage spools. Venusian air is directed to a portion of the tape's surface where component particles are deposited, and the feed spool is actively driven by a motor to move the sampled tape Section forward and create a time- and altitude-synchronized record of Venusian aerosols. The tape essentially acts as a conveyer belt to place sample directly under a knife edge instrument inlet. An elevator-style sealing mechanism is actuated to create a knife edge seal, with the tape acting as a gasket. At this point another sample may be collected, and the sampling process repeated. A schematic of this design concept is shown in Figure 13.

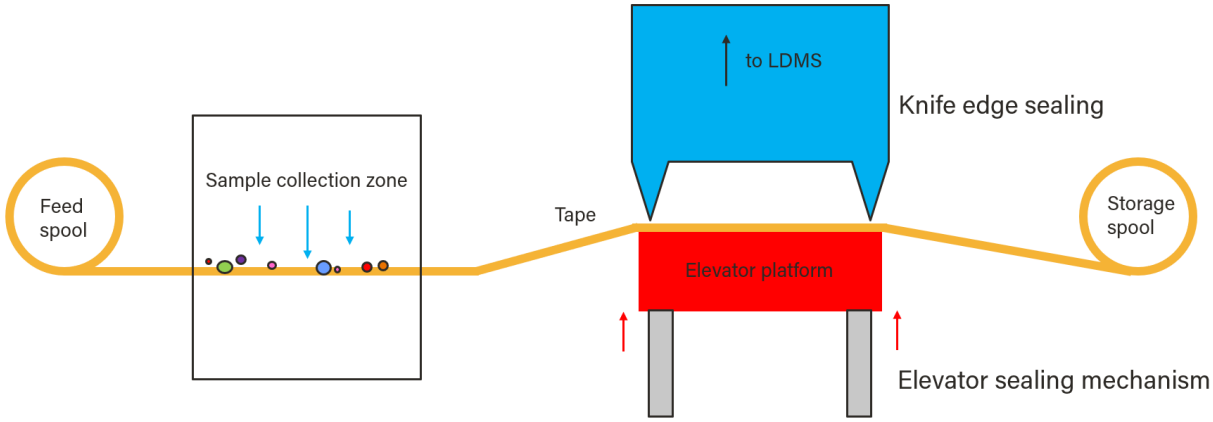

Figure 13: Illustration of the concept of an all-in-one collection, delivery, and sealing mechanism for in situ LDMS (example instrument) analysis.

This concept is based on the Precision Subsampling System (PSS), a previous HBR design created for use with a time-of-flight mass spectrometer (TOF-MS) developed by Will Brinckerhoff at the Goddard Space Flight Center (GSFC) [22]. In this system, select portions of a heterogenous rock core are powdered by a subsampling device. The rock cuttings are collected on Kapton tape and, using the paired spools approach, are moved to the knife edge inlet of the instrument. An elevator sealing mechanism is used to create a knife edge seal, with the Kapton tape acting as the gasket. The design and prototype system are pictured in Figure 14.

Method In order to advance this sample delivery concept for a future flight mission to Venus, HBR

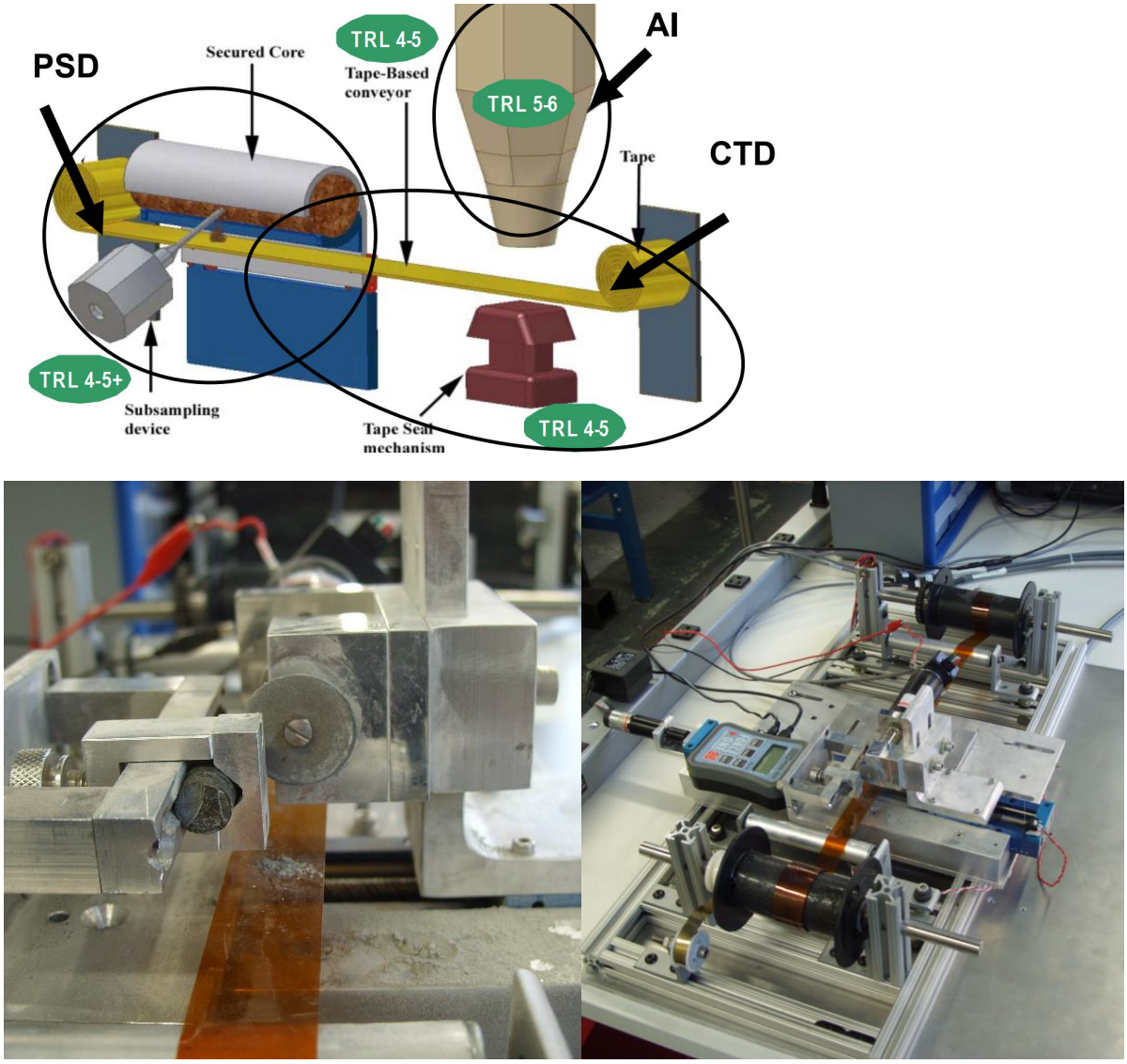

Figure 14: Top: Schematic arrangement of the main PSS components, showing notional concepts for mounting a core sample, extracting and collecting fines, and transport/interface to an analytical instrument (AI) enabled by a seal made with sample substrate tape. Current technology readiness level (TRL) of key subsystems is shown. (Brinckerhoff et al. 2010) Bottom: Honeybee-built prototype of the PSS.

has developed the design of a prototype that can be used in laboratory testing. Rather than include

space for an arbitrary in-line instrument, this design has a cut-and-release mechanism to eject the storage spool for sample return. In addition to validating the feasibility of the overall concept, the primary goal of a test campaign using this prototype would be to determine the capture efficiency of atmospheric particles. This is important to validate experimentally because there is limited research to draw upon and it is challenging to model. Further, bounding the capture efficiency is a critical part of sizing a future flight-forward design to ensure that enough sample is captured within the time, mass, and power constraints of the reference mission. Other

goals of the test campaign for which this prototype would be used are to determine how strongly sulfuric acid adheres to the tape, sulfuric acid removal strategies, and the scientific value of a spool returned to Earth with Venusian particles embedded in this manner.

Key Results The main result is the prototype design. There are three key elements of the prototype design that need to be created with sufficient fidelity such that test results can be used to inform a future flight-forward design: the sample tape, sample delivery, and spool ejection mechanisms. These elements are what the prototype design testing would seek to better characterize and refine, and thus are described in greater detail in this Section. To enable all the testing goals described in subsection 4.1, the prototype design also aims to be made from COTS components that are easily acquired and modular so that it remains flexible and easy to iterate upon as testing progresses.

The most important element to replicate with high fidelity in the prototype design is the tape itself, which acts as both the sample capture surface and conveyer belt. While many different material candidates are possible for the tape, a gold foil (that is not “sticky” like traditional tape) has been selected in this design. This selection is due to its material compatibility with both the instrument and Venusian atmosphere, its malleability, and high free surface energy, which attracts particles. To this end, Honeybee, per recommendation from NASA JPL used gold in the witness plate assemblies (WPA) on the Mars 2020 sample return [23]. The Honeybee WPAs are shown in Figure 15.

Another key design element is the sample delivery system that deposits material on the gold surface. Low power passive methods of collection or faster and higher power active methods are both compatible with the design concept, but to enable fast and efficient laboratory experiments, an active system was chosen. For an active system, two approaches can create airflow: “pushing” air using a fan, or “pulling” air using a vacuum pump. A fan was the preferred selection for a prototype given the ease with which flow rate and air flow angle/direction can be modified for different experiments. However, with a fan, air must pass through blades which will intercept some aerosols and change its performance. To minimize this effect, a “Dyson-style” fan can be used, where the majority of air flow is induced through an open ring. While there are no COTS solutions for this type of fan in this size, a simple housing design enables the user to connect any COTS fan to the prototype to create this style of induced-flow fan. Preliminary calculations indicate that readily available COTS fans meeting the packaging requirements could provide approximately 5 x 10^8 particles per hour from an environment simulating the Venusian clouds upper haze (estimated particle density of 500 particles/cm^3). This serves as a starting point for integration of a fan into the design.

The final key element to be tested is the storage spool eject mechanism. HBR designed an eject mechanism compatible with this sampling concept and feasible with remote operations on Venus. Once the feed spool has been completely unwound and cannot be driven any further, a frangible nut releases a spring-loaded mechanism. This mechanism thrusts the storage spool forward, where it could be grabbed by a robotic arm, mating device, or in the case of the prototype, removed by hand. The tape is inherently taut between the two spools, and the ejection of the storage spool causes the loose end of the tape to be sliced by a sharp edge on the housing, enabling release from the rest of the system.

Surrounding these three key design elements are the supporting mechanical design elements. For

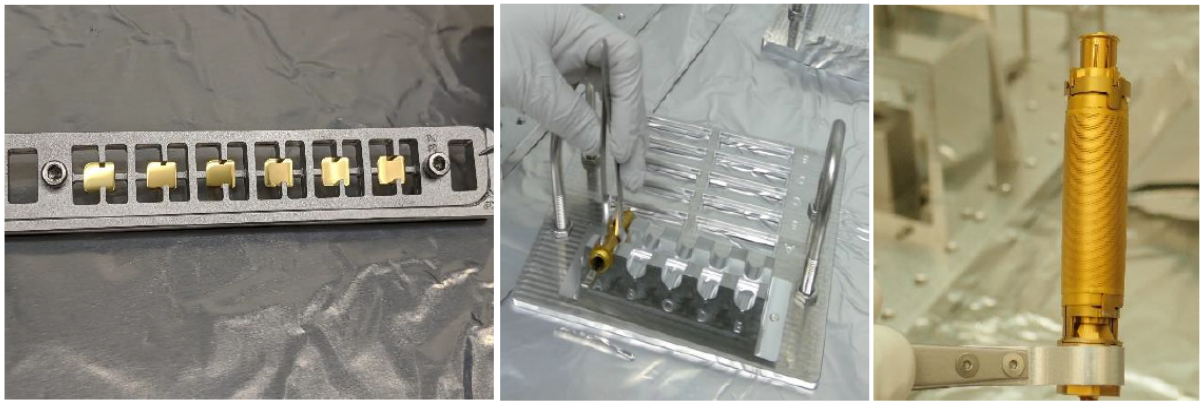

Figure 15: Mars 2020 Left- gold witness plates, Middle- aluminum witness plate, Right- TiN-coated particle sieve.

the purposes of the prototype, the drive and storage spools can be rapidly manufactured and connected with a COTS drive belt that can be driven by a DC motor. An in-line tensioner ensures that the gold tape always remains taut between the two spools. The entire assembly is mounted to a base plate so that it is easy to transport and so that components are easy to replace for different testing needs. Material selection for the prototype depends upon whether it will be used with sulfuric acid or an atmospheric simulant. The integrated prototype design is shown in Figure 16.

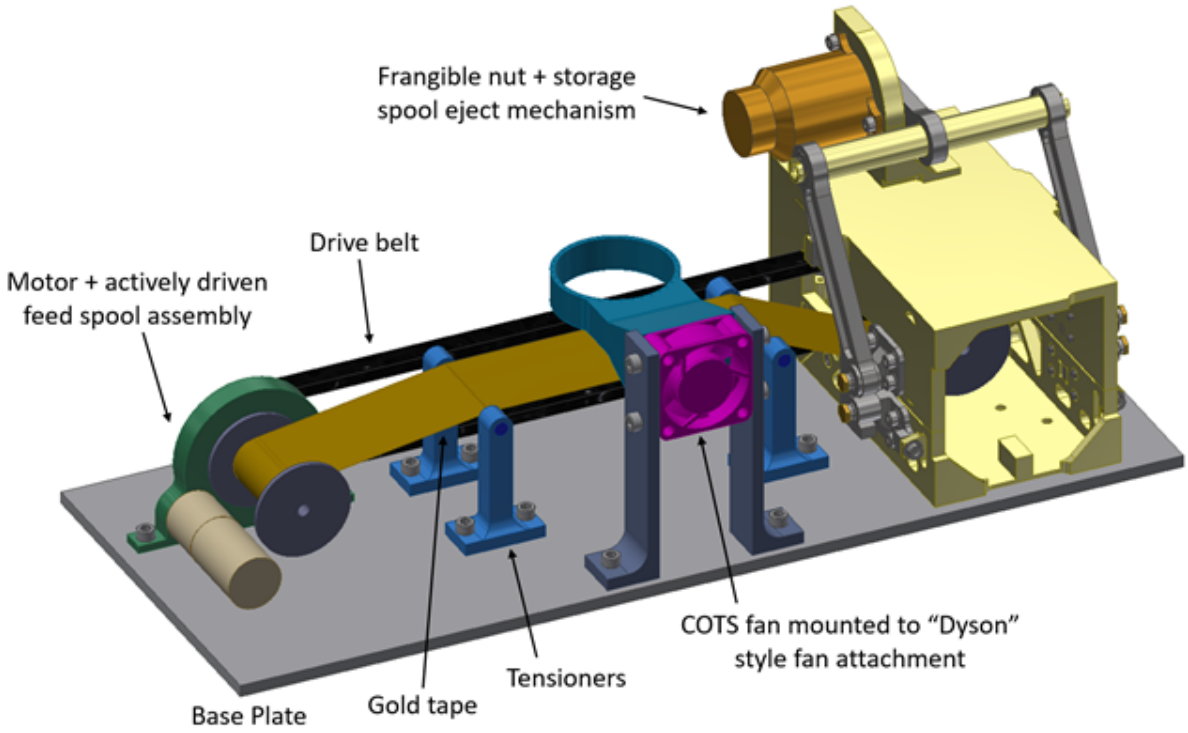

Figure 16. Diagram illustrating key components of prototype design

4.2 Liquid Sample Collector

4.2.1 Sample Flow and Collection Model

Goal Develop a model of particle flow in order to determine whether an active or passive sampler (or both) are needed to capture an adequate volume of Venus cloud particles during the mission lifetime.

Background info The cloud particle size spectrometer experiment on the Pioneer Venus mission documented liquid particles' density and mean diameter inside three cloud layers [19] (Table 8).

Method Our model determines the number of particles of different diameters by random sampling from the aerosol distribution [24]. The particle density is then combined with the sample collection efficiency of our collector designs as a function of the particle diameter. With this model we compared a constant balloon ascent and a variable balloon ascent collection campaign.

Our model is driven by the size and distribution of aerosols in the Venusian cloud deck as assessed by the particle size nephelometer of Pioneer Venus, and aerosol collection efficiency vs. particle diameter models. The Venus aerosols can be modeled as consisting of three modes, although all modes are not present at all altitudes. Modes 1 and 3 particle distributions are modeled as lognormal whereas the Mode 2 particle distribution is taken as Gaussian distribution. We combine

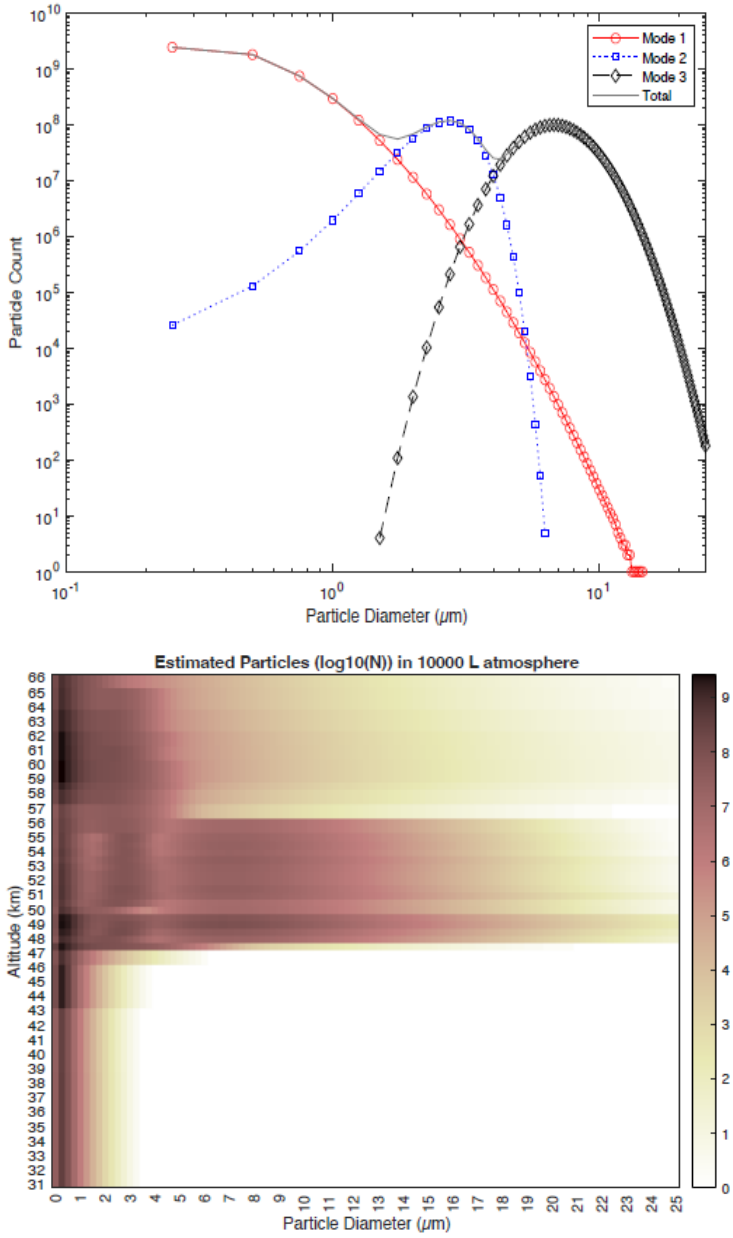

Figure 17. Aerosol particle size distribution. Left: Example distribution at 50 km. The x-axis is the particle diameter and the y-axis is the number of particles. The particle density distribution is shown for the Mode 1, 2, and 3 particles and the total number of particles. Right: The particle density in a 10000 L atmosphere volume. The x-axis is the particle diameter and the y-axis is the altitude above the Venus surface from 31 to 66 km.

random sampling and approximate method using cumulative distribution function to obtain number of particles within a particle size bin (Figure 17).

We investigated two active collectors which use liquid impingement for capturing aerosols: (1) the SASS 2400 with 40 L/min air processing capability and (2) the SASS 2300 with more than 300 L/min air processing capability. We also investigated two passive collector designs: (1) A “Fog harp” collector with a wire mesh design and (2) A “kirigami” collector that has cuts and folds in a metal sheet instead of a metal wire mesh. For each collector a collection efficiency vs particle diameter curve was defined based on empirical and/or theoretical data in the literature. An example of collection efficiency curves is shown in Figure 18. For passive collectors, where collection is dependent upon the wind speed, we assume winds sampled from empirical Vega measurements in combination with balloon ascent-generated local wind. An overview of the model is shown in Figure 19.

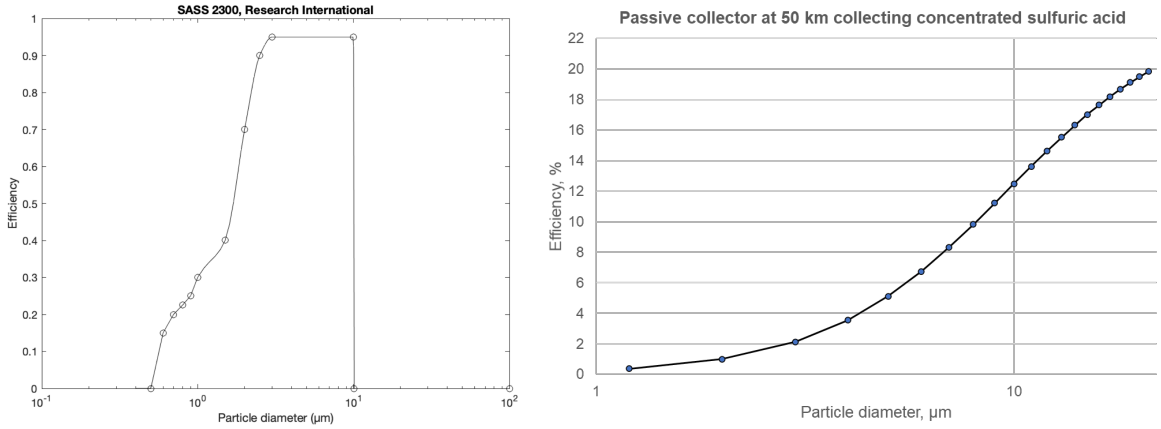

Figure 18. Collection efficiency of particle collectors. The y-axis is collection efficiency and the x-axis is particle diameter. Left: The SASS 2300 Active Collector. Right: The passive fog harp collector (this work).

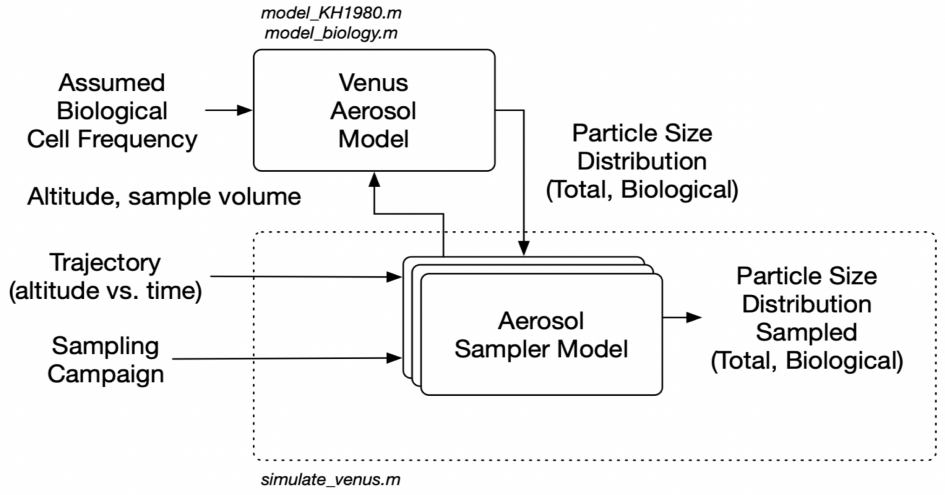

Figure 19. Simulation approach for estimating the collected sample amount at various altitudes.

Key finding As an example of model application, consider the average size and distribution of cloud particles in various layers, shown in Table 8. In one day of flight through the clouds, approximately

$7.78 \cdot 10^6$ liters of atmospheric volume is swept by the fog collector (30x30 cm^2 collector and assuming an average vertical wind speed of 1 m s^{-1}).

Cloud layer, km	Particle modes	Mean density, cm^{-3}	Mean size, µm	Particles per ml	Liquid availability during sweep flight with 30x30 cm collector, ml/day	Estimated collection, ml/day
Upper 66-56	U-Mode 1	333	0.35	$4.45 \cdot 10^{13}$	2	0.2–0.5
	U-Mode 2	45	2.2	$1.79 \cdot 10^{11}$		
	U-Mode 3	—	—	—		
Middle 56-50	M-Mode 1	97	0.3	$7.07 \cdot 10^{13}$	57	5-15
	M-Mode 2	38	2.7	9.7^{10}		
	M-Mode 3	33	7.4	$4.71 \cdot 10^9$		
Lower 50-48	L-Mode 1	432	0.4	$2.98 \cdot 10^{13}$	159	15-40
	L-Mode 2	65	2.5	$1.22 \cdot 10^{11}$		
	L-Mode 3	102	7.2	$5.12 \cdot 10^9$		

Table 8. Top-down estimate of the collection rate of liquid droplets by deposition using passive and electrostatic collectors. According to [24,25]*, the Mode 3 particles include non-spherical particles, which might indicate its solid nature.*

Using the bottom-up modeling approach (Figure 19), we found that the fog collectors can process larger volumes under reasonable conditions than the active collectors (sometimes called powered liquid impingers) and at likely much lower power (Figure 20). Although the active collectors can in some cases achieve higher efficiency, the fog collectors can process 1-2 orders of magnitude more particles and collect equal or more particles than the active collectors. We note that the collection amount for the fog harp is linearly proportional to the collection area and wind speed.

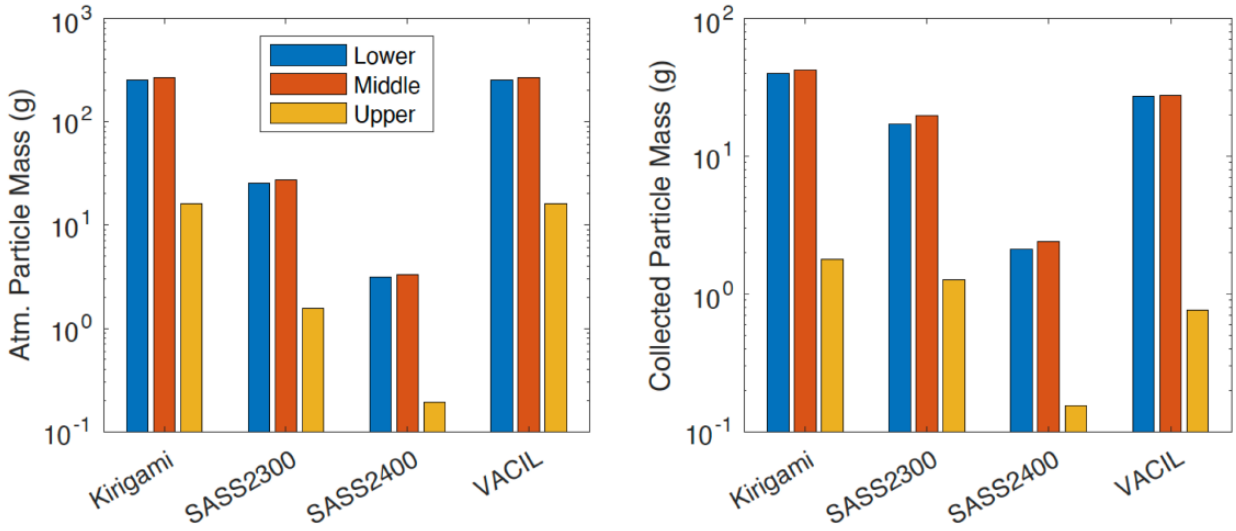

Figure 20. Comparison of active and passive liquid collector amount. The x-axis shows the four collectors analyzed. Left: The y-axis shows the mass of the liquid particles processed. Right: The Y=y-axis shows the mass of the collected samples. The fog harp collects equal to or more than the SASS because it is able to process a larger volume of the atmosphere due to large collection area and vertical wind speeds. (VACIL - Venus Aerial Collector Instrument for Liquids, our proposed fog harp collector described below).

We found that a variable ascent CONOPS that spends more time in the lower clouds collects mores sample than a constant ascent (Figure 21). Our current estimates yield that a wire mesh "fog harp" can collect up to 25 mL of sample in the lower cloud layer and about 16 mL in the middle cloud layer.

Volume (mL)

Region	Constant	Variable
Upper	0.428	0.341
Middle	15.6	16.6
Lower	15.2	25.7

Mass (g)

Region	Constant	Variable
Upper	0.761	0.607
Middle	27.6	29.4
Lower	27.0	45.7

Figure 21. Sample amount collected for a variable ascent sampling campaign.

4.2.2 "Fog Harp" Collector Design and Prototype

Goal Investigate passive aerosol collector designs and design a prototype. Develop collection efficiency models to feed in to the sample collection model.

Background info Collection of liquid particles on another planet has never been demonstrated previously and requires dedicated development.

Passive collectors have relatively low collection efficiencies (i.e., 1–5%) of fog-like particles due to added factors of shedding rate (when particles reach the critical size, they shed to the collector by gravity) and aerodynamic deviations. We investigated collecting the liquid sample by depositing aerosol droplets on a metallic mesh. The mesh geometry is beneficial because it reduces the deviation of the incoming flow and therefore increases efficiency. The shedding rate can be manipulated by changing the thickness of individual wires and mesh-formation geometry. On the other hand, surface fraction of wires on the mesh has to be around 50% for the maximum shading coefficient. The Stokes number, shown in Equation 1 for a simple single wire case, characterizes

the ability of a particle to follow streamlines: at a low Stokes number, the droplet collision with the wire will be minimal since it will follow streamlines. At a high Stokes number, the trajectory is drag-forceless, and droplets are targeted toward the wire; however, it requires a very fine mesh. The Stokes number is:

$$S_t = \frac{2 \times R_d^2 \times \rho_w \times U}{9 \times \eta_g \times R_c} \quad (1)$$

where R_d is the droplet radius, ρ_w is the droplet's composition density, U is relative velocity, η_g is atmospheric viscosity, and R_c is wire radius.

Key findings Although the passive collector is a simple solution, the efficiency is limited. We nonetheless built a prototype of a passive collector (two types, a wire-based and a kirigami design) (Figure 22). The current preliminary design employs 900 cm^2 nickel-copper alloy square mesh. The single wire diameter is 0.7 mm, and the average wire separation is 2.5 mm, providing 60% of the open area. The metallic mesh is acid resistant but requires erosional testing in 100°C concentrated-sulfuric-acid medium. Preliminary, the erosion rates of the nickel-copper alloy are known from literature and are expected to be limited to the values provided in the Table 9 [26].

Sulfuric acid concentration	Approximate erosion rate at 60°C, mm/year	Approximate erosion rate at 95°C, mm/year
20%	0.3	0.3
40%	0.2	0.4
60%	0.2	0.4
75%	1.5	2.7
96%	3-3.5	4

Table 9. Approximate erosion rates of the deposition mesh at various sulfuric acid concentration and temperatures [26].

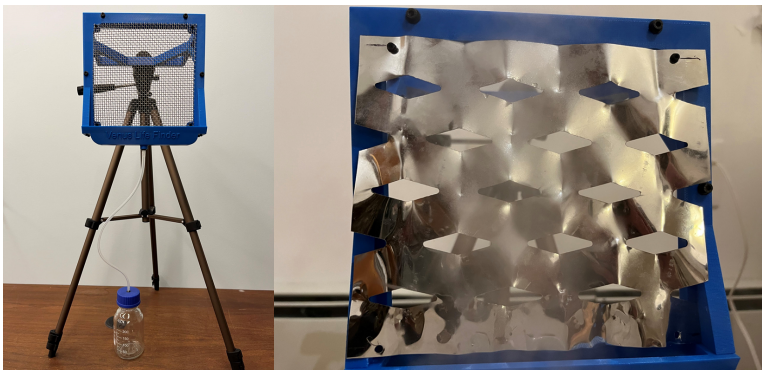

Figure 22. Aerosol collector prototypes. Wire mesh design (left) and kirigami design (right). Each prototype is approximately 6x6 inches in size. A humidifier was used to send water vapor droplets to the aerosol collector. The water droplets were shed by gravity down to the trough then a tube into the

collection bottle. Wire mesh collection rate is approximately 10 mL/h and kirigami is 3-4 mL/h under the conditions tested.

We estimated the collection efficiency of the wire mesh collector (Figure 23). The efficiency is a function of wire radius, liquid droplet density, relative airspeed, atmospheric viscosity, and the shedding rate.

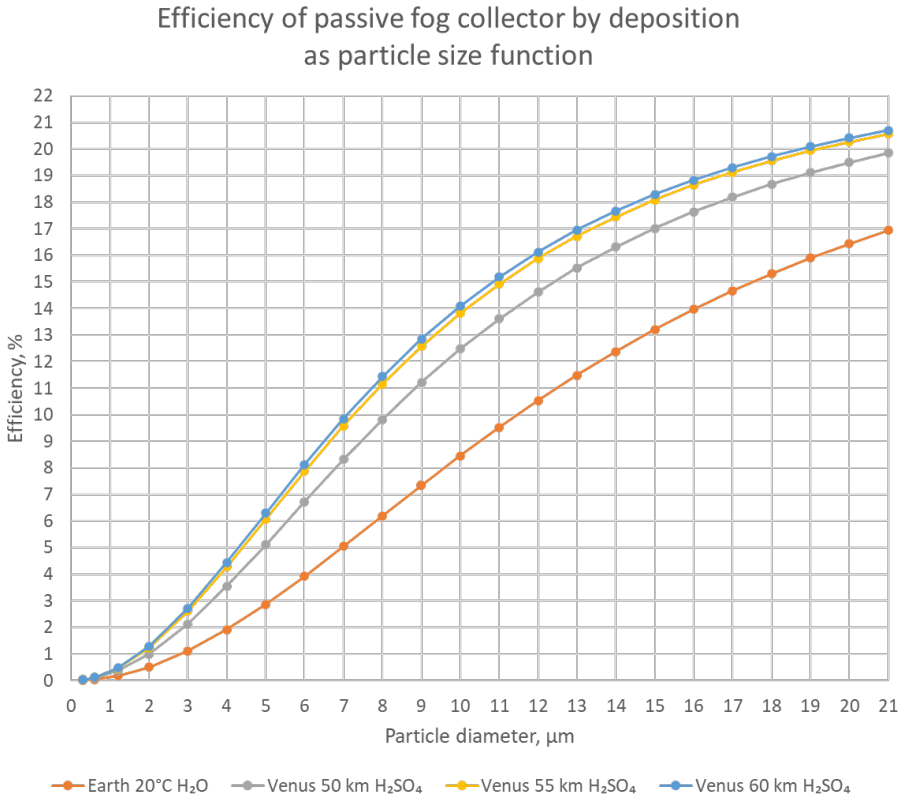

Figure 23. Collection efficiency of the fog harp collector. The x-axis is the particle diameter and the y-axis is the percentage efficiency of collection. The efficiency is higher for sulfuric acid droplets compared to water. We see that the collection efficiency increases for higher altitude due to lower temperature, which causes changes in viscosity.

An electrostatic collector can be used to increase collection efficiency by overcoming the drag force. If one ionizes the incoming cloud with an emitter electrode to a few kilovolts and keeps the metallic conductive mesh at ground, the resulting Coulomb force would drive significantly more droplets to a collision trajectory with mesh. This will require under 1 W of electrical power, but the ionization process might alter potential biological cells if there are any. However, it is expected that the efficiency of the collection would increase to 25% and more in comparison to the passive collection of 1-10%; moreover, the electrostatic collection would collect submicron particles, which is not feasible for the passive wire-based collector.

We created a preliminary design for an electrostatic collector (Figure 24). Once the droplet grows large enough to shed by gravity, it will move toward the sample concentration area, which will transfer the sample to three parallel pipes. Afterward, the distribution system will move the sample to the storage vials. The sample collection confirmation will be achieved by either (i) a microfluid counter built into the distribution system or (ii) a conductivity wire inside the vial. Multiple pipes are used to avoid the risk of clogging a single pipe and to reduce the risk of contamination by having triplicate samples from similar environmental conditions. However, the negative side of such a

setup is required prolonged exposure periods in order to collect a sufficient amount of material. Figure 24 shows simplified schematics of the deposition-based collector. We note that this system can operate as both passive and electrostatic; the former requires the activation of a high-voltage supply and charging of the conductive wires on the inlet. The efficiency can be increased further by having two meshes sandwiched with a small separation gap. During the mission cruise, the system would need to be sealed by the hatch, which will be opened before the collection phase. The vial carousel will be placed in a sealed, contamination-free area. We plan to test the 1 kV electrostatic fog harp during the Phase II study.

Despite the promise of the electrostatic aerosol collector, more work needs to be done for collection of submicron-sized particles.

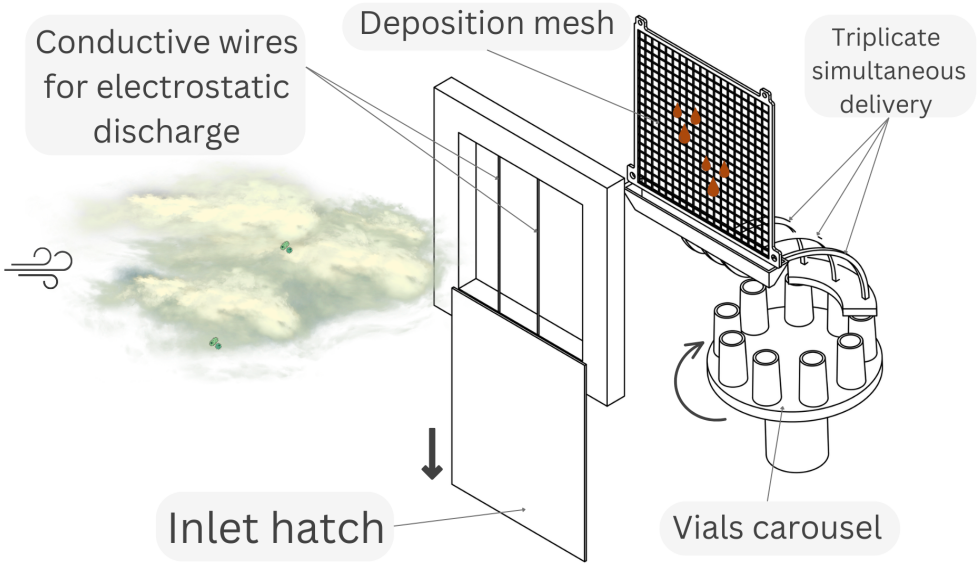

Figure 24. Preliminary schematic of liquid collection by deposition onto an electrostatically charged collector.

5 Venus Ascent Vehicle

Novel Result: *Launch from an aerial platform in a remote planetary atmosphere has not been done before. We found that a two-ton rocket can launch the ~10 kg sample return canister into a low Venus orbit and fit within a feasible closed mission design.*

The Venus Ascent Vehicle (VAV) will transfer the sample canister from balloon platform to the orbit of Venus for return to Earth. Although launch from an aerial platform in a remote planetary atmosphere has not been done before, there are some Earth examples to consider. Specifically, Northrop Grumman's Pegasus rocket at 18,500 kg was launched from an aircraft at 12 km. Virgin Orbit launched the 30,000 kg (~30 tons) LauncherOne rocket from 11 km altitude. These aircraft are very stable with accurate positioning, as compared to a balloon. Interestingly, the company Zero2Infinity plans to use a balloon to lift a "Bloostar" rocket to 20 km for launch. However, the 100 m/s (220 mph) winds on Venus, and lack of navigation aids, create very different constraints for atmospheric launch from those on Earth.

5.1 VAV Comparison with Mars Ascent Vehicle

The launch of a rocket from an extraterrestrial body has been achieved by the Apollo Lunar Module (LM) and the Chang'e-5 ascender launched from the surface of the Moon. There is no significant atmosphere on Moon which greatly reduces the launch risks and improves performance. Moreover, the LM and Chang'e-5 were launched from steady ground whereas the VAV will be launched from a balloon platform in dynamic wind conditions.

In 2028, the Mars Sample Return campaign will be launched to Mars, which will include a Mars Ascent Vehicle (MAV). The MAV will provide heritage for some subsystems or their components such as avionics, RCS, thermal control, and systems integration and testing as well. We use the MAV as a reference for these subsystems. Although there are some similarities between MAV and VAV, they differ vastly in scale and launch conditions. Table 10 compares the MAV and VAV to emphasize the challenges unique to Venus and other solar system bodies with a substantial atmosphere.

Parameters	**MAV**	**VAV**
Launch ΔV	~5 km/s	~9 km/s
Payload to orbit	16 kg (MPA + OS)	16 kg (SC + PA)
Entry deceleration load	15 g	36 g
Thermal environment	Constant temperature maintained during cruise and surface storage, 16 heater zones, along with passive insulation	Might need both active heating and cooling, depending on CONOPS
Pressure at launch	~0.01 bar	~0.2 bar
Launch mechanism	Toss-up in the air using springs	Release from the balloon
Launch conditions	Stable lander platform	Clouds, winds and gusts, sulfuric acid
Knowledge of launch conditions	Orbiting assets and higher fidelity atmosphere models	Local conditions measured, higher uncertainty and variability, wind shear
Launch g-load	5 g lateral load	40 g axial load

Table 10. Comparison of the Mars Ascent Vehicle and the Venus Ascent Vehicle.

5.2 VAV Sizing and Trade Studies

Goal Determine the VAV mass and volume to inform the balloon platform design and overall mission launch feasibility.

Method We conducted several trade studies to select the baseline design in the mission concept. The following figure lists the design options for the VAV with the selected options highlighted in green.

Propulsion	Solid	Hybrid	Liquid
Stages	Single	Two-stage	Three-stage
Launch Altitude	60-63 km	64-67 km	68-70 km
Launch Method	Drop from balloon and launch	Point and launch from balloon	
Thermal Control System	A protective container around VAV	TCS integrated with VAV	

Figure 25. Trade study options of the critical VAV parameters.

5.2.1 Launch altitude and VAV configuration selection

Goal Select optimal VAV launch altitude.

Background Information The selection of the launch altitude depends on two competing factors: the final mass delivered to orbit and the mass and size of the balloon envelope. As the altitude increases, the density of the atmosphere decreases. As a result, the ΔV required for launch decreases, and more mass is delivered to orbit for the same VAV configuration. But because of the lower density, the balloon envelope needs to be larger to be able to lift the same VAV mass. Thus we perform this trade study to minimize the total aerial platform mass, i.e. balloon and VAV total mass.

We considered the launch altitude from 60 km to 70 km. The cloud region of interest is up to 60 km for sample collection. Beyond 70 km, the balloon envelope is too large. An initial trade study with simplified assumptions found that there are no significant mass benefits to the VAV beyond 67 km. Following that, we did a higher fidelity modeling of the VAV ascent trajectory and varied the launch altitude from 60 to 67 km.

Along with the launch altitude, the VAV mass is also dependent on the propulsion type and the number of stages. Here we describe the two trades and the candidate configurations chosen for the subsequent analysis.

Method

Propulsion. We considered three propulsion types: solid, liquid, and hybrid. The Table 11 compares the advantages and disadvantages of the three propulsion types. Solid and liquid are well-understood technologies and have extensive flight heritage for Earth launch systems. Hybrid, on the other hand, is a developed technology but does not have a flight heritage. Although hybrid propulsion has higher efficiency, the Isp is about 300 s which does not provide sufficient mass benefits due to higher dry mass compared to solid propulsion. Therefore, we choose solid and liquid propulsion for further quantitative analysis.

	Solid	Liquid	Hybrid

Advantages	● Simple, no moving parts ● Extensive spaceflight heritage ● Little preflight checkout ● No leak, spill, or slosh ● Can be stored for 5 to 25 years ● Can be throttled, stopped, or restarted a few times if preprogrammed	● Thrust is controllable ● Higher Isp ● Storable liquid propellants can be stored for several years	● Solid fuel and liquid oxidizer ● Controlled combustion
Disadvantages	● Explosion and fire potential are larger ● Grain damage can occur due to temperature cycling or rough handling ● Integrity of grains is difficult to determine in the field ● Larger dispersion in final orbit	● Relatively complex design ● Tanks need to be pressurized ● Spills or leaks can cause fire ● Sloshing in tanks can cause flight instability ● Cryogenic propellants cannot be stored for long periods without high power	● Relatively complex design ● Not a huge advantage in overall mass

Table 11. Comparison of advantages and disadvantages of the solid, hybrid, and liquid propulsion systems.

Stages. We evaluated different configurations of the VAV from single-stage-to-orbit to three-stage. Single-stage launch vehicles are not viable for solid and hybrid propellants due to the high ΔV requirements. A liquid single stage using hypergolic propellant, for example, MMH fuel and N2O4 oxidizer have a Gross Lift-Off Mass (GLOM) of more than 3000 kg.

Trajectory Optimization. We optimized the launch trajectory of the VAV to maximize the final mass in orbit. GPOPS-II optimization software is used [27]. The three parameters that are varied for the trade study are propulsion, stages, and launch altitude. We mainly looked at three VAV configurations: (1) 2-stage solid; (2) 3-stage solid; and (3) 2-stage with a liquid first stage and solid second stage. The Venus Global Reference Atmospheric Model (GRAM) was used for pressure, density, and wind profiles. The Cd of the rocket as a function of the Mach number is referenced from Sutton [28]. The speed of sound profile as a function of altitude is referenced from [29].

For solid propulsion, we adopted the Star solid rocket motors from Northrop Grumman. Star motors use Hydroxyl-terminated polybutadiene (HTPB) for fuel.

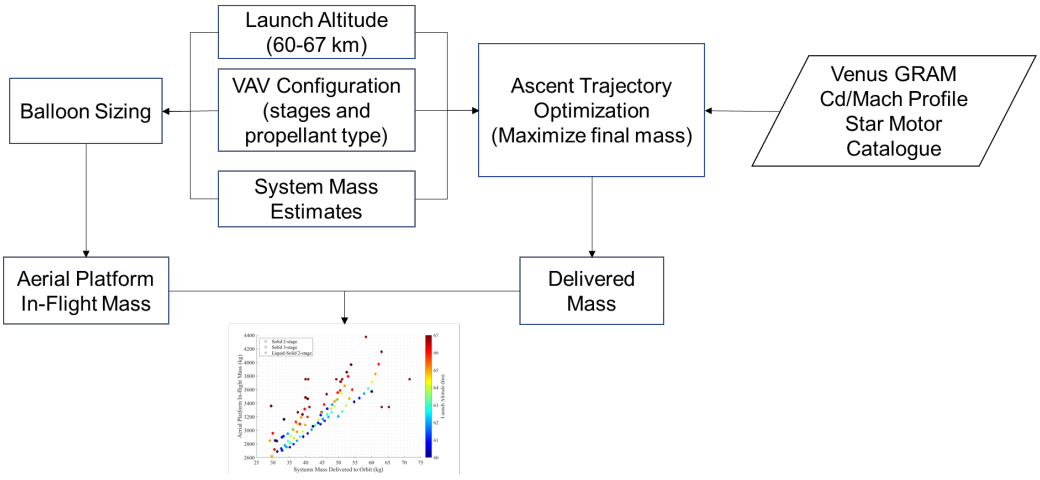

Figure 26. Block diagram of the method used for performing VAV and balloon trade study and sizing.

The pitch angle of the VAV is the control parameter. For each configuration, trajectories are generated for various launch altitudes and GLOM. Figure 27 shows optimization results for the selected baseline case (60 km launch altitude, two-stage solid rocket).

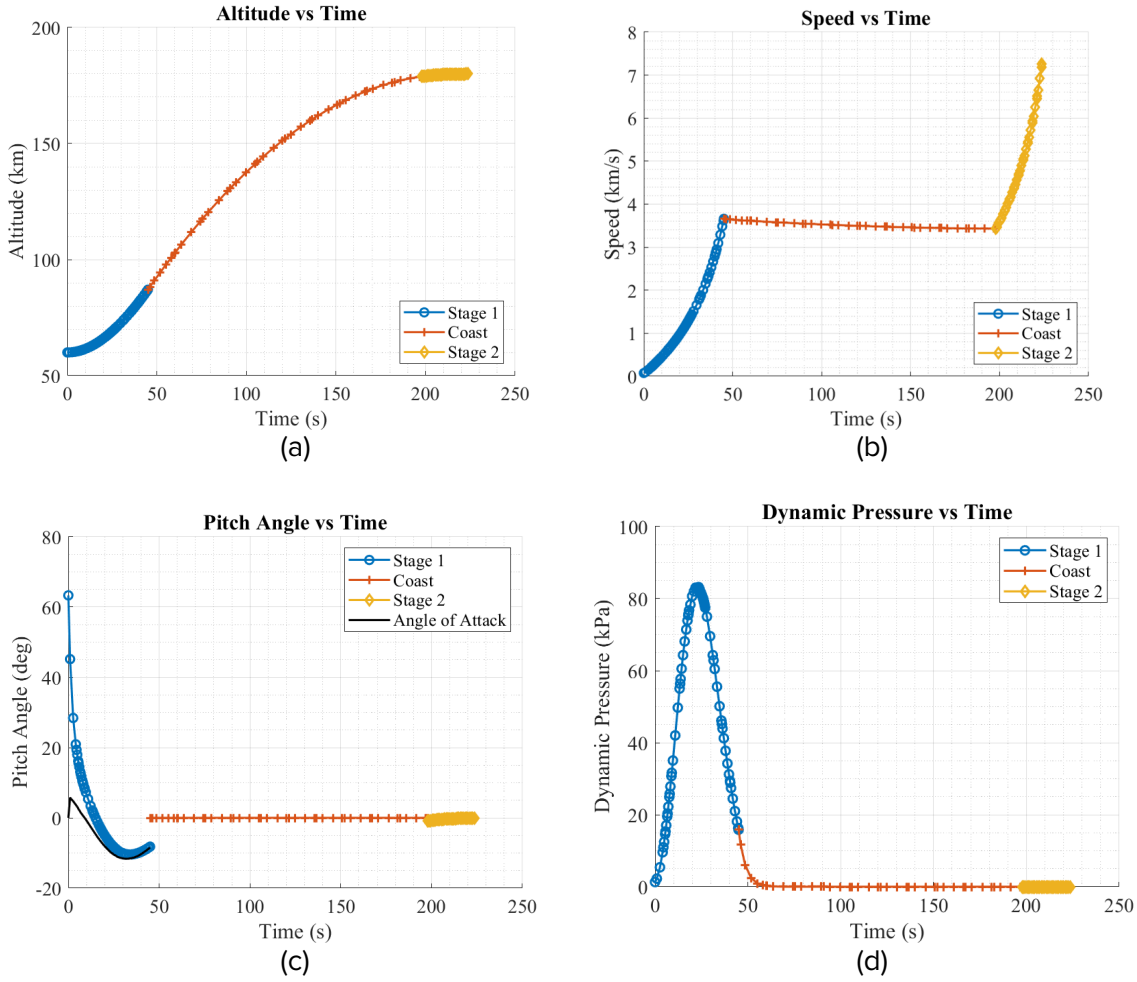

Figure 27. VAV trajectory optimization result for the baseline case: two-stage, solid motor, launched from 60 km altitude. X-axis is time from launch in seconds. (a) Y-axis is the altitude of VAV in km. (b) Y-axis is the speeds of VAV in km/s. (c) Y-axis is the pitch angle control value in degrees. (d) Y-axis is the dynamic pressure experienced by VAV during ascent.

We plot the aerial platform mass (balloon + gondola) vs the mass of the system delivered to orbit. The system here includes SRC, RCS, avionics, structure, and payload adapter. We choose this metric because all these subsystems are payload for the final stage and the mass estimates can be improved further.

Key Results The key results of the trade are:

1. For every 1 kg increase in mass delivered to orbit, there is a 30 kg increase in the aerial platform mass.
2. The optimal launch altitude range is 60 to 63 km.
3. Liquid propulsion does not provide significant mass benefits as compared to solid propulsion

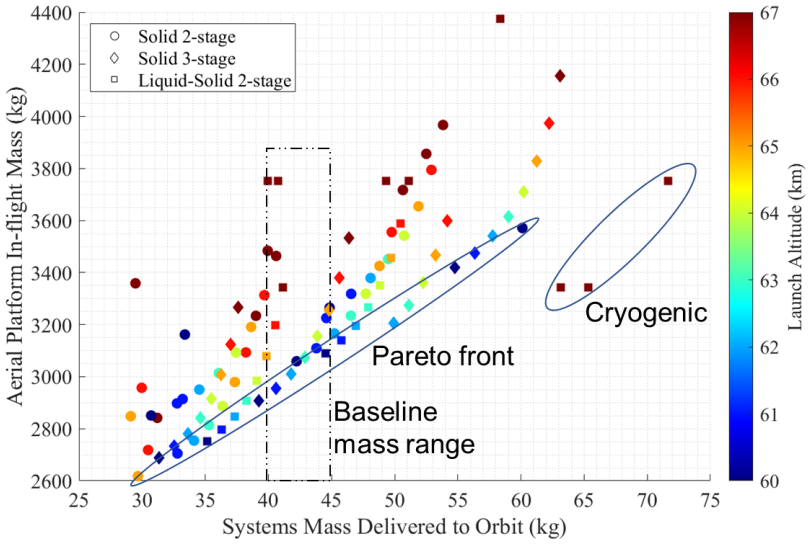

Figure 28. Aerial platform sizing for various VAV configurations and launch altitudes. Y-axis shows the total balloon plus VAV mass and x-axis shows the mass of the system delivered to the orbit. The color of the data point indicates the launch altitude. The dotted rectangular box indicates the baseline range of mass of the systems (sample canister, avionics, payload adapter, RCS). The oval shapes highlight the Pareto front of the graph, showing that the suitable launch altitude is between 60–63 km.

We choose a two-stage solid rocket motor configuration for the VAV. The launch altitude is 60 km. The mass breakdown of VAV is given in Table 12.

System/Component	Mass (kg)	Reference
Stage 1 Motor Dry Mass	97	Star 31
Stage 1 Propellant	1286	
Thrust Vector Control	10	
Aft Compartment	8	Max axial load of 39 gs, aluminum
Interstage	3	
Stage 2 Motor Dry Mass	31	Star 30 BP - reduced propellant
Stage 2 Propellant	340	
Forward Compartment	5	Max axial load of 39 gs, aluminum
RCS	10	Mars Sample Return MAV
Avionics	10	
Payload Adapter	8	
Sample Canister	10	
TPS	7	Total heat load 1.3 kJ/cm2

Total Estimated	**1824**	
VAV Max Possible Value	**1837**	
Margin for delivered systems	**13**	**30.70%**

Table 12. Mass breakdown of the Venus Ascent Vehicle.

5.2.2 VAV Thermal Control System

We present a qualitative assessment for choosing the VAV's Thermal Control System (TCS) for the baseline mission. The solid rocket motor has a storage temperature range of -6°C to 37°C. The temperature of Venus's atmosphere ranges from 93 °C at 48 km to -11 °C at 60 km. The TCS should maintain the storage temperature of the VAV within its recommended range to prevent thermal cycling and cracks in the propellant. There are two options for the TCS design: (1) An enclosure and (2) Integrated TCS. The enclosure is a similar concept to the thermal 'igloo' design for the MAV. It makes the system modular and less complex at the cost of higher mass. On the other hand, an integrated TCS is mass efficient but requires advances in thermal protection material and coatings on the surface of the VAV that are restaurant to sulfuric acid and protective covers for the solid motor and RCS nozzles that can be easily removed by the exhaust from the nozzles. We choose the integrated TCS option due to its mass efficiency. Such a TCS is an innovative solution for planetary launch systems that can benefit missions beyond the Venus sample return.

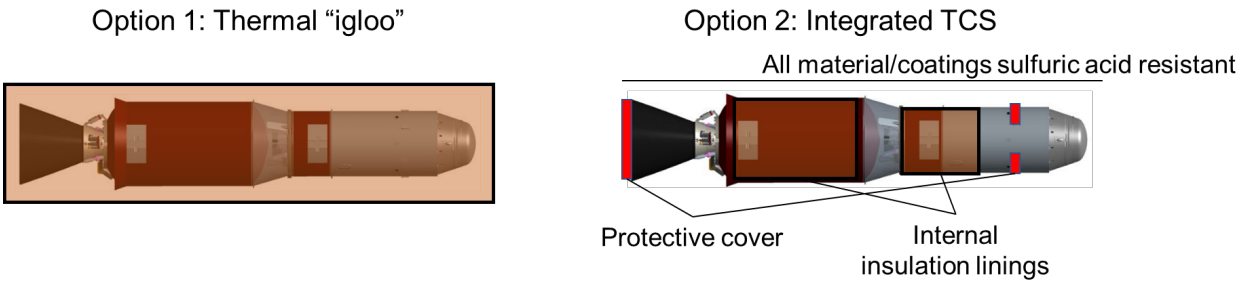

Figure 29. VAV thermal control system options.

5.3 VAV Technology Challenges

TRL Assessment: The VAV is a highly complex system designed by integrating various subsystems. Therefore to assess the TRL of the VAV, we break down the system into some of the key and most complex subsystems and assess their TRL individually. Table 13 lists the subsystems and our assessment of the current TRL.

Subsystem	TRL	State-of-the-art
Solid rocket motor	4	Star motors in kick stages
Thrust Vector Control	4	Star motors with Thrust Vector Control
GNC	1	Basic principles and parts of the technology identified. Feasibility not proven.
Thermal Control System	2	Thermal igloo for MAV
Launch System	4	Pegasus, Bloostar, SAID demonstration

Table 13. Technology Readiness Level of critical subsystems of the Venus Ascent Vehicle.

5.3.1 Key Areas to be Addressed

Guidance, Navigation, and Control

The VAV needs to be injected into a predictable orbit, which requires precise guidance, navigation, and control. However, there is a lack of aids for navigation and attitude determination on Venus because the clouds block the sun, stars, and terrain, and no magnetic fields are present. In other words, conventional star trackers, magnetometers, sun sensors, and Terrain Relative Navigation are not feasible. We can use the basic principles of Doppler and range measurement and build on existing methods for deep space navigation, augmenting them to be used in real-time.

The radio link between the VAV and orbiter can be used to measure position, velocity, and attitude. The measurements can be augmented with an Inertial Navigation System (INS). For Venus, a proposed method using a single orbiter link for real-time tracking [30] uses a two-way ranging and Doppler coupled with barometric altitude measurement. For a chosen frozen orbit the positioning accuracy is shown to be 95 m with a 1-sigma error of 75 m.

For attitude determination, a potential method is to use a direction-of-arrival (DOA) technique, which determines the direction of the receiving radio signal with respect to an array of antennas on the VAV (see Figure 1 in [31] for a schematic of a satellite-ground station system). The preliminary analysis by [31] shows an RMSE error of less than 0.1° for a signal-to-noise ratio better than -6 dB and DOA sampling greater than 50 in a given time frame. The balloon and DSN can also be employed as additional references.

The coverage provided by the orbiter is critical for the accuracy of the state determination. Multiple orbiting beacons could be required as communications relays, thereby increasing the mass and cost of the mission. Orbit selection is crucial to maximize navigation coverage for a single pass, provide numerous VAV launch opportunities, and minimize ΔV for orbit transfer to rendezvous with the VAV.

These techniques can be built on well-established methods used on Earth with existing capabilities. The INS is used on Earth for aircraft and military applications with high precision. For example, a Ring Laser Gyros (RLG) has bias stability of less than 0.01 deg/hr and noise of less than 0.01 deg/root-hour [e.g., Honeywell's GG1320AN]. Nonetheless, the drift grows over time for the integrated velocity, position, and attitude measurement. Typically, on Earth, the INS is augmented with other sources of absolute state measurement such as GPS, compass, visible and infrared star sensors, and radar. For Venus, the INS needs to be augmented with novel techniques of state measurement for initial state information input.

For position and velocity determination, the Doppler and range method has long been employed for deep-space navigation. Radiometric data is integrated over several hours, days, or weeks and combined with a high-fidelity orbit determination model [32]. For example, the Very Long Baseline Interferometry (VLBI) was used for tracking the VEGA balloons but is not a real-time method [33]. The viability of a single orbiter to provide navigation support on Venus has also been studied, but not in real-time [34]. For attitude determination, the radio link between the orbiter and balloon/VAV can be used. A method using doppler measurements was used by the MSL and Mars 2020 teams to measure the attitude of the cruise vehicles [35,36]. But this method is not real-time and relies on the slow and predictable change in the spacecraft's attitude. The DOA method of attitude determination is not in use for spacecraft due to other methods available such as sun and star sensors, but the basic principles are established and application concepts exist [37].

Atmospheric Dynamics Considerations

The atmosphere of Venus, particularly the cloud layers and upper atmosphere, have wind speeds ranging from 70 m/s to 100 m/s in the East-West direction, also called zonal winds. The wind speed increases with altitude and changes direction as well leading to extremely high wind shears. On Earth, launch vehicles are not launched in such weather conditions.

Apart from the zonal winds, there are North-South and vertical winds that vary with altitude, latitude, and local time as well [38]. The North-South winds are observed to increase with latitude and are believed to be caused by the Hadley cell circulation and solar thermal tide. These meridional winds are towards the north in the northern hemisphere and towards the south in the southern hemisphere. Therefore, it is desirable to deploy and launch from the equatorial region.

There are disturbances caused by various types of waves observed on Venus, including gravity waves and convective motions. Gravity waves are caused by mountains and propagate upwards leading to vertical velocities of 0.5–5 m/s. Therefore, it is desirable to launch from a region above plains and avoid highlands such as Aphrodite Terra for the VAV launch phase.

Using the current knowledge of the atmospheric dynamics of Venus, we can narrow down the relatively stable regions to launch the VAV. But there are still disturbances and wind shear that may not be possible to avoid. Such conditions can lead to high loads on the VAV during ascent and risk structural failure. Another risk is that of the trajectory of the VAV drifting and leading to either failure of orbit injection or large deviation in the injected orbit.

There is a need to model these uncertainties to determine the range of performance of the VAV and determine the requirements for its structure and control subsystem. Large uncertainties will require larger safety and mass margins in the design.

6 Balloon Platform

Novel Result: *No prior studies have focused on a variable altitude science mission balloon that can also carry a two-ton launch vehicle. We designed a simple and mass efficient single-envelope balloon that uses ballast for ascent rate control. We found that a very large balloon—on the order of ~30 m in diameter—is required to support the payload gondola as well as the two-ton VAV rocket. Providing further challenge, the ~7000 m^3 balloon envelope needs to inflate within ~30 minutes, about 40 times faster than the 15m^3 Vega balloons.*

The mission concept includes a variable altitude balloon that allows sample collection from different cloud layers during the ascent from an initial 48 km minimum float altitude. At the end of the sample collection phase, the balloon will continue upwards to ~60 km for the VAV launch.

While balloon-born atmospheric science is common on Earth, there is no detailed recorded heritage for application of a balloon-based aerial platform at another planet. Indeed, the only past planetary balloon missions are the Russian Vega mission [39,40]. The Vega balloons were 3-m diameter fixed-altitude whereas our mission aims for ~30 m diameter variable altitude.

Goal Develop a concept for the balloon platform to carry the VAV and operate with other mission elements. Specify the balloon requirements and explore feasibility of variable altitude balloon

options for competing properties for sample collecting mobility and heavy lift/high altitude VAV delivery.

Method Trade studies were performed to identify balloon technology that could fulfill the Venus Sample Return mission requirements. Primary requirements driving the down-select are:

1. *Elevated Temperature Environment*
Ability to withstand 48km Venus altitude ambient temperature of 92° C, and ~110° C accounting for balloon envelope absorptivity/emissivity (α/ε).

2. *Sulfuric Acid Environment*
Ability to withstand the Venus atmosphere sulfuric acid environment

3. *Lifting Gas Retention*
Lifting gas retention is of critical importance for mission survivability—particularly in view of the dramatic increase in gas permeability of barrier membranes with increasing temperature: At the maximum operational temperature of 110° C, an approximate 100-fold increase in barrier permeability is anticipated.

4. *Robust Strength*
Robustness and strength are intertwined: the balloon envelope must display sufficient loadbearing strength for its 2-ton payload while resisting a broad spectrum of mission-related abuse such as tight folding and packaging, deployment misalignment, opening shock, flutter and "flagging" during initial inflation under parachute descent, variable inflation pressure etc. Robustness is the ability to maintain the requisite lifting gas retention in the face of traumatic operational parameters such as (a) environmental variables (radiation, sulfuric acid, temperature extremes and variability, etc., (b) physical variables (creasing, fatigue, and impact, and (c) general temporal degradation.

5. *Low Mass (Low Specific Energy Containment)*
Common to all space exploration, the Venus Sample Return mission seeks the lowest possible mass and stowed volume.

6. *Manufacturability*
The preceding requirements demand incorporation of highly sophisticated materials that are exceptionally challenging to work with and integrate. As such, a balloon architecture and design that supports incorporation of such material assemblies is a critical requirement.

Balloon Types and Assessment Summary
Balloon type candidates were assessed based on previously identified relevance to Venus exploration. Three primary balloon architectures comprising five individual architectures (Figure 30) were considered during the down-select effort:

1. *Single Envelope:* Single envelope balloons present the simplest, most predictable option for high-mass payloads. Venus sample return requires a gradual, one-way ascent from 48 to 52km, then continuing to VAV launch at 60km. Such single-pass altitude control is best serviced by precision ballast drop, reversely attenuated, if needed, by lifting gas venting. Due to the volume-to-surface area advantage of larger volumes, single envelope balloons also benefit from lower envelope mass than segmented configurations such as the motorized designs below (2a, and to lesser extent 2b). Two designs:
    a. *Conventional Gore-based (Vega mission type)*: Gore-based architectures (Figure 30, top left; Figure 31, left) do not facilitate fabrication/incorporation of the complex material layups needed to fulfill the mission requirements.

b. *Thin Red Line UHPV* [1]: Contrasting with gore-based designs, UHPV fabrication is entirely planar (Figure 30, top center; Figure 31, right) supporting highly complex material assembly.

2. *Active (motorized) Altitude Control:* Motorized Altitude Control balloons are designed to repeatedly traverse a prescribed altitude range. Active motorization provides accurate, responsive control, but comes at the cost of technological complexity and additional mass. These systems are best suited to repeatedly and accurately traverse a prescribed altitude range. Motorized systems were hence ultimately disqualified from the down select.
    a. *Mechanical Compression*: (Figure 30, right) High temperature adaptability, therefore suited to traverses of low- to mid- altitudes (40-60km). Rapid maneuverability.
    b. *Pumped Helium*: (Figure 30, bottom center) suited to higher altitude traverses (52-70km) due to helium pump sensitivity to elevated temperatures.

3. *"Light Bulb":* The Light Bulb is a hybrid Single Envelope/Mechanical Compression design. The large upper segment provides the majority of the lift, while the stack of small bottom segments provides mechanical compression altitude control capability. The trade found that the range of altitude provided was far from sufficient for the desired 48 to 60 km.

6.1 Balloon Type Down-select Conclusion

The Single Envelope UHPV (1b) was down-selected as best option for the Venus sample return mission for the following reasons:

1. Simple, planar design supports complex, high performance material assembly.
2. Operationally robust and tolerant of manufacturing variance.
3. UHPV-specific attributes confirmed by NASA studies:
    a. Lowest mass containment architecture.
    b. Structurally determinate isotensoid architecture always assumes the same geometry regardless of size, pressure, or deflective external loads.
    c. Predictably and inexpensively scaled to any size. Burst pressure can be accurately predicted—regardless of size. Sub-scale testing is predictive of larger scale architectures.

[1] Ultra-High Performance Vessel

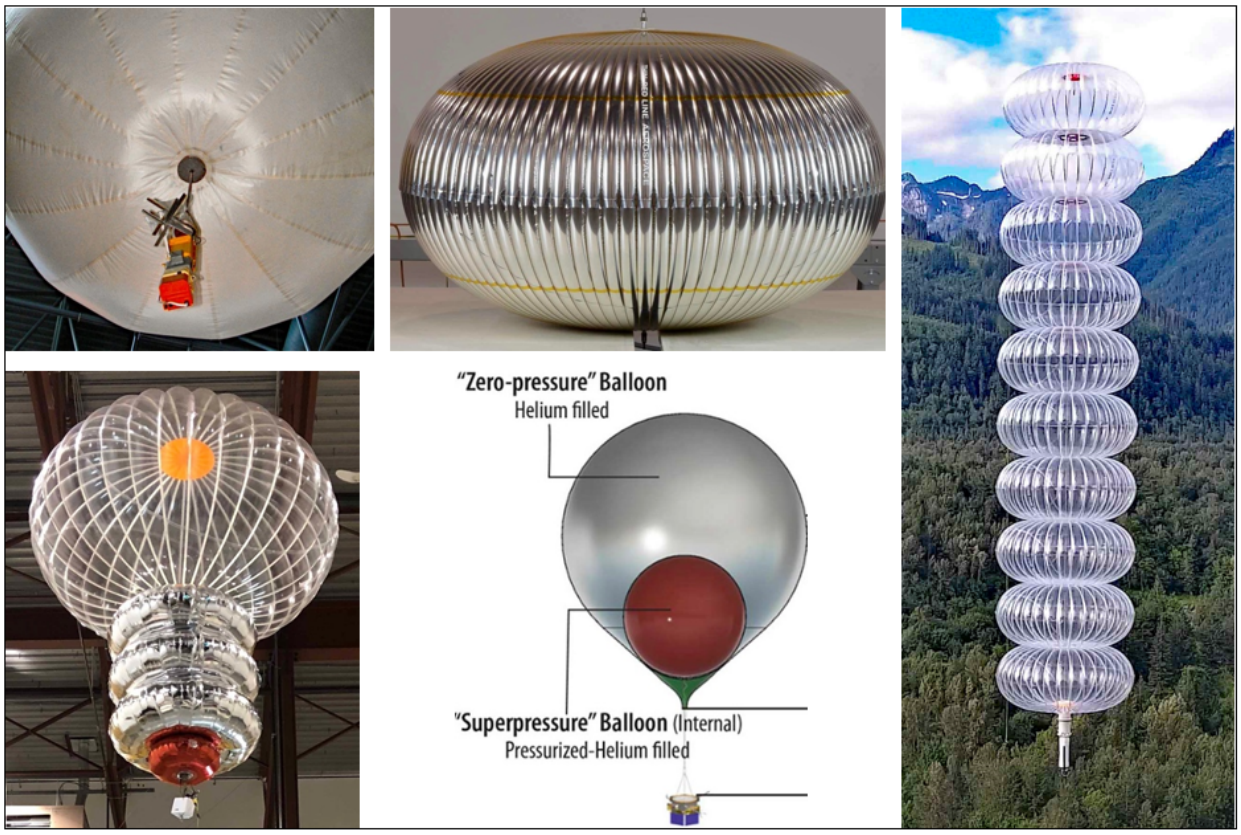

Figure 30. Balloon type down-select. Clockwise from top left: Single Envelope: Conventional gore-based (Vega Venus balloon); Single Envelope: Thin Red Line UHPV Venus prototype; Motorized: Thin Red Line Mechanical Compression Altitude Control; Motorized: Pumped Helium Altitude Control; "Light Bulb" Thin Red Line Hybrid Single Envelope/Mechanical Compression.

Figure 31. Comparison of traditional gore-based balloon fabrication and TRLA's planar fabrication. Top: Gore-based fabrication. Bottom: UHPV planar fabrication.

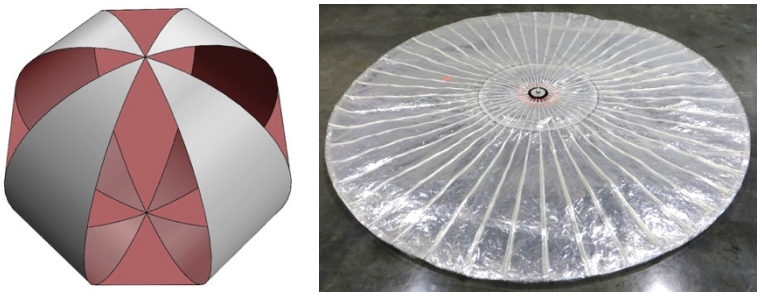

6.2 VAV Launch Altitude Selection

We integrated the balloon sizing estimates for various launch altitudes and gondola mass values with the VAV sizing (Section 5.1.1). The launch altitude is a critical parameter for the balloon volume and envelope mass (Figure 32). We note that apart from the mass of the balloon envelope, the volume of the balloon is also an important consideration as it directly affects the inflation rate requirement and the complexity of packaging and deploying the balloon.

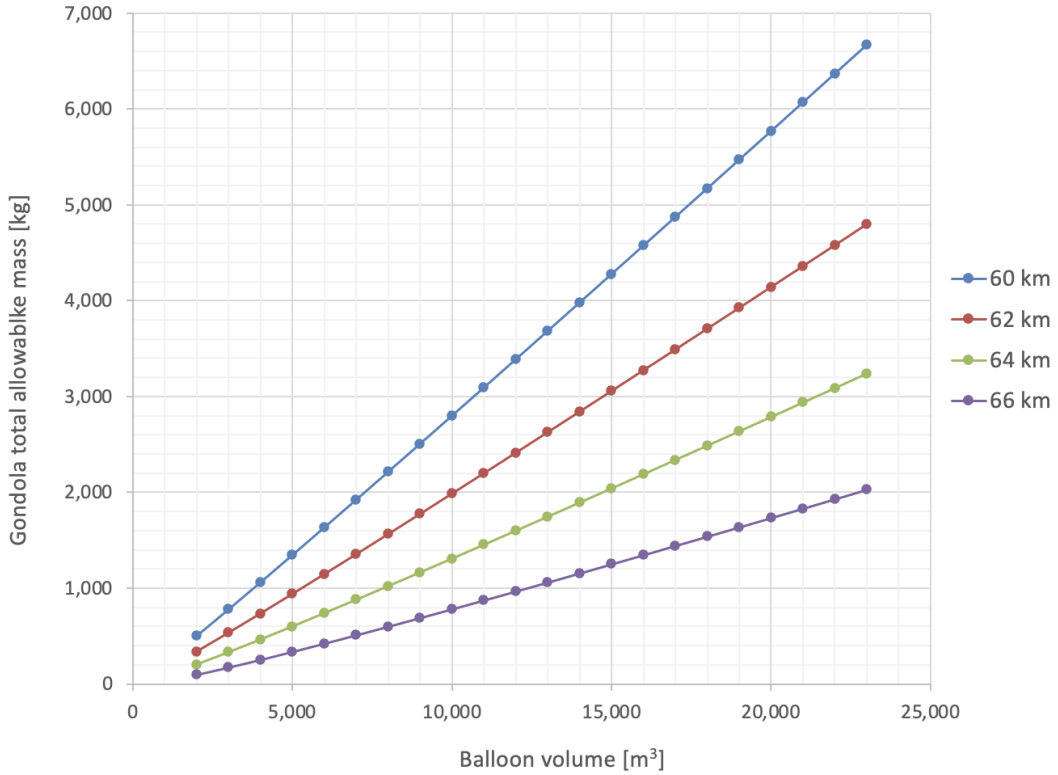

Figure 32. Balloon volume as a function of gondola mass and launch altitude. The x-axis is the balloon volume in cubic meters. The y-axis is the gondola mass in kg, and the different curves are for launch altitude. The higher altitude the launch, the larger the balloon has to be.

6.3 Balloon Technology Challenges

Rapid inflation during descent through the atmosphere

The exceptionally high payload mass for the Venus sample return mission demands a much larger balloon than previously contemplated for any Venus mission. Upon release of the mission's flight system from its atmospheric entry aeroshell container, parachutes are deployed to further slow descent of the flight system while simultaneously setting the stage for balloon inflation. As the system descends under parachute, rapid inflation of the balloon is critically important to ensure that the flight train does not descend to altitudes presenting dangerously high temperatures prior to achieving stable, controlled flight. This mission stage is doubly critical because of the high payload mass. The primary challenge is how to transfer the exceptional amount of helium to the balloon envelope in the shortest possible time. While the inflation time window can be expanded by slowing descent with a larger parachute, parachute mass increases rapidly to become unsustainable in the global mission context.

In addition to the feasibility of rapid expansion, there are challenges due to the dynamics of system during descent. High-volume, rapid inflation of a flaccid balloon is fraught with exceptional risk of trauma to the balloon envelope caused by flow volume venturi effects and whip-like behavior of inflation tubes. Furthermore, upward propagation of inflation gas bubbles through the folds of the partially inflated balloon may exacerbate traumatic aerodynamic instabilities during descent and/or, at worst, destroy the balloon.

Several potentially damaging aerodynamic instabilities confront the aerial platform flight train during its descent under parachute and throughout the initial balloon inflation phase. Of particular concern are (a) oscillations in the parachute caused by vortices shed from the suspended inflating balloon, (b) differential "spinnakering" of areas of flaccid balloon envelope leading to envelope trauma due to "flagging"; and resulting from the preceding, (c) off-axis perturbations of the descending flight train.

These challenges need to be addressed in the development of the balloon platform technology for sample return. We plan to address some of these in Phase II.

7 Dynamics of Aerial Platform System

Goal Determine the magnitude of pendulum-like motion of the balloon-VAV system and evaluate control feasibility for VAV launch.

Background information The Venusian zonal winds at 60 km near the equator have an average speed of 70 m/s. But there are variations in wind speeds locally and possibly wind gusts. We baseline the expected vertical gust magnitude in reference to the data from the Vega balloons, although we note that the Vega balloons floated near 53 km altitude whereas the VAV launches from 60 km. The Vega balloon instrument suite recorded vertical wind gusts ranging from 1–3.5 m/s in magnitude [41]. A constant downdraft of 2 m/s was recorded for Balloon 2 towards the end of its trajectory, which is attributed to it passing over the 5-km-high Aphrodite Terra. This pass is also conjectured to cause a northward excursion at a speed of 3.5 m/s.

Method We modeled the balloon-gondola systems as a series of three rigid links connected by ideal spherical joints. The balloon and gondola are modeled as rigid bodies and the tether as two rigid spheres connected by a massless inextensible line. Figure 33 shows the schematic of the system, which has a total of 12 degrees of freedom. We model the balloon as a rigid spherical shell and the gondola as a uniform cylinder. The detailed modeling method and simulation results are given in [42].

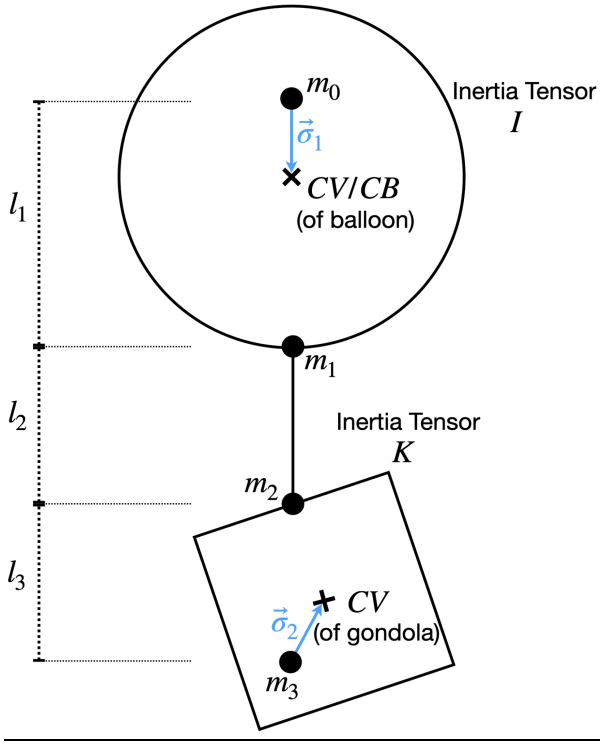

Figure 33. Balloon-gondola system schematic for modeling [42].

Key Results Because of the large mass of the vehicle relative to anticipated gust magnitudes, the system behaves sluggishly in response to downdrafts. Elevation and spin rate of the gondola are highly subdued. Even in the absence of friction, typical spin rates do not exceed 10^{-7} deg/s under downdraft conditions. Figure 34 shows that, given an initial elevation of 1 deg, the amplitude of the gondola response is quite steady under a 100–second gust with a maximum magnitude of 3.5 m/s. Such disturbances can be feasibly controlled using existing technologies on Earth for pointing balloon-borne telescopes.

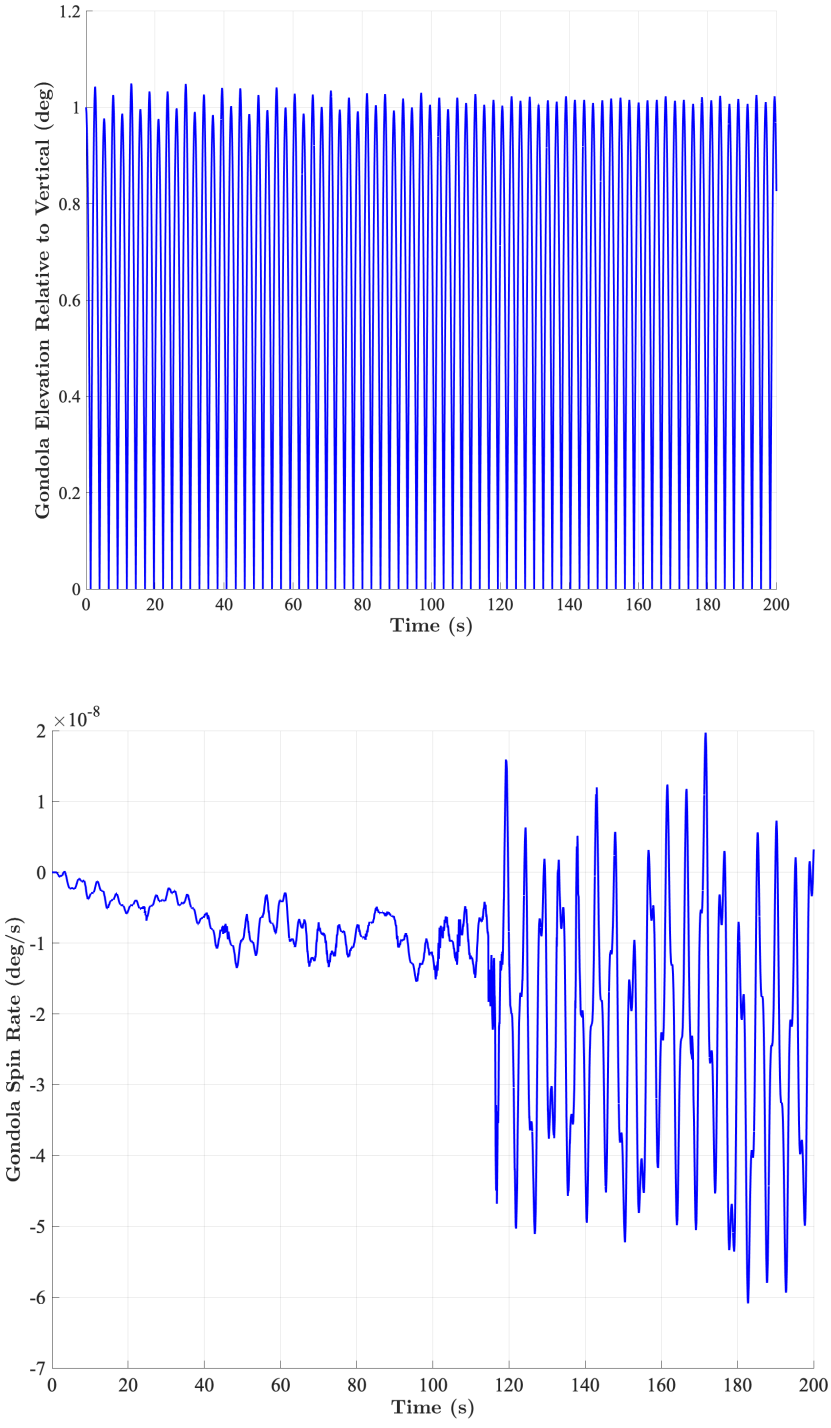

Figure 34. Gondola elevation and spin rate response to wind gust. The x-axis is time in seconds. Top: Elevation angle on the y-axis. Bottom: Spin rate of the gondola on the y-axis. The simulation is for 200 seconds initiating with a 100-second downdraft with a maximum magnitude of 3.5 m/s. The elevation response is steady over the simulation period and the gondola spin rates are negligible.

Future work Regarding the dynamical response of the gondola to wind perturbation, aerodynamic torque on the gondola depends on the displacement of its centers of mass and volume, which were assumed to coincide in the initial analysis. Regarding attitude determination and control, more work is needed to determine the appropriate attitude determination system for the gondola. Balloon-borne telescopes often determine their attitudes using Sun or star sensors, which may be occluded in the Venusian cloud environment.

8 Technology Gaps, Spin-offs, and Synergies

Table 14 provides a preliminary list of technologies that are critical for the Venus atmospheric sample return mission. These technologies are not only crucial for our specific mission, but have commonalities across other missions. There are gaps in enabling technologies for example balloon packaging for the interplanetary cruise which is crucial for aerobot missions to atmospheric bodies. Although many of the integrated systems are unique to our mission, for example, VAV is designed for the Venusian environment, the subsystems have synergies beyond the mission such as an integrated thermal control system or navigation in a low visibility environment. We have proposed to address some of these gaps in Phase II and design a technology development roadmap.

Technology	**State-of-the-Art**	**Commonalities Across Other Missions**			
		Sample Return	**Planetary Exploration**	**Venus Exploration**	**Synergies on Earth**
Entry and descent system	Rigid aeroshells	✓	✓	✓	✓
Balloon aerial deployment and inflation	Slower inflation rates demonstrated	(✓)	(✓)	✓	
Balloon packaging	Vega balloon	(✓)	(✓)	✓	
Balloon material with high dynamic load limits	None	(✓)	(✓)	✓	
Navigation without visual references or magnetic field	Basic Principles	✓	✓	✓	✓
Launch vehicle control in unpredictable and turbulent weather	None	(✓)		(✓)	✓
Balloon-borne rocket launch mechanism	Sub-orbital on Earth	(✓)		✓	✓
Space grade materials compatible with hot sulfuric acid for prolonged exposures	Industrial grade materials available			✓	
Aerosol sample collection	Conceptual designs	(✓)	(✓)	✓	✓
Sample handling and storage	Dry soil samples, MSL, Mars2020, Osiris-Rex, etc.	(✓)	(✓)	✓	
Sample transfer	MSR Sample Transfer Arm	✓			
Sterilization protocols for astrobiology	In situ exploration protocols. None for Venus.	(✓)	(✓)	(✓)	

Sample Return Container	MSR, Hayabusa	✓			
Earth re-entry vehicle	Stardust, Osiris-Rex, MSR	✓			

Table 14. Key technologies and commonalities across various missions. (The (✓) indicates relevant to bodies with dense atmosphere).

9 Conference Presentations Relating to NIAC Phase I Study

1. I. Iakubivskyi, et al. “Venus Life Finder Missions: Sampling Collection Strategy." Finnish Satellite Workshop 2023 with Finnish Remote Sensing Days and URSI National Convention, 18-20 January 2023, Finland. (Poster)
2. S. Seager, “Venus as a Potentially Habitable Planet”, MAVEN Team Meeting, Boston, MA, 14 November 2022.
3. I. R. King, K. Bywaters, K. Zacny, S. Seager, et al. “Prototype Design of a Flexible Tape and Roller Sampling System for Venusian Atmosphere Aerosol Capture and Delivery.” 20th Meeting of the Venus Exploration and Analysis Group, November 7-9, 2022.
4. R. Agrawal, S. Seager, J. J. Petkowski, et al. “Venus Atmospheric and Cloud Particle Sample Return for Astrobiology.” Venus Science Conference, September 29th, 2022.
5. S. Seager, J. J. Petkowski, S. Saikia et al. “*In Situ* Missions to Study Venus as a Potentially Habitable Planet.” Venus Science Conference, September 29th, 2022.
6. J. J. Petkowski, S. Seager, P. Klupar, C. E. Carr, D. Grinspoon, B. L. Ehlmann, S. J. Saikia, R. Agrawal, W. Buchanan, M. U. Weber, R. French, S. P. Worden. “Venus Life Finder Mission Study.” Astrobiology Science Conference, 15-20 May 2022, Atlanta, GA (abstract + talk).

List of Acronyms and Abbreviations

CONOPS	Concept of Operations
DOA	Direction of Arrival
EDI	Entry, Descent, and Inflation
GLOM	Gross Lift-Off Mass
HBR	Honeybee Robotics
LSC	Liquid Sample Capture
MAV	Mars Ascent Vehicle
MSR	Mars Sample Return
PSS	Precision Subsampling System
RCS	Reaction Control System
SHS	Sample Handling System
SLS	Space Launch Systems
SRC	Sample Return Canister
SSC	Solid Sample Capture
TCS	Thermal Control System
TRL	Technology Readiness Level
UHPV	Ultra-High Performance Vessel
VACIL	Venus Aerial Collector Instrument for Liquids
VAV	Venus Ascent Vehicle
VFA	Variable Float Altitude
WPA	Witness Plate Assemblies

References

1. Seager, S.; Petkowski, J. J.; Gao, P.; Bains, W.; Bryan, N. C.; Ranjan, S.; Greaves, J. The Venusian Lower Atmosphere Haze as a Depot for Desiccated Microbial Life: A Proposed Life Cycle for Persistence of the Venusian Aerial Biosphere. *Astrobiology* **2021**, *21* (10), 1206–1223.

2. Limaye, S. S.; Mogul, R.; Smith, D. J.; Ansari, A. H.; Słowik, G. P.; Vaishampayan, P. Venus' Spectral Signatures and the Potential for Life in the Clouds. *Astrobiology* **2018**, *18* (9), 1181–1198.

3. Mogul, R.; Limaye, S. S.; Way, M. J.; Cordova, J. A. Venus' Mass Spectra Show Signs of Disequilibria in the Middle Clouds. *Geophys. Res. Lett.* **2021**, e2020GL091327.

4. Rimmer, P. B.; Jordan, S.; Constantinou, T.; Woitke, P.; Shorttle, O.; Paschodimas, A.; Hobbs, R. Hydroxide Salts in the Clouds of Venus: Their Effect on the Sulfur Cycle and Cloud Droplet PH. *Planet. Sci. J.* **2021**, *2* (4), 133.

5. Bains, W.; Petkowski, J. J.; Rimmer, P. B.; Seager, S. Production of Ammonia Makes Venusian Clouds Habitable and Explains Observed Cloud-Level Chemical Anomalies. *Proc. Natl. Acad. Sci.* **2021**, *118* (52).

6. Petkowski, J. J.; Seager, S.; Grinspoon, D. H.; Bains, W.; Ranjan, S.; Rimmer, P. B.; Buchanan, W. P.; Agrawal, A.; Mogul, R.; Carr, C. E. Astrobiological Potential of Venus Atmosphere Chemical Anomalies and Other Unexplained Cloud Properties. *Astrobiology* **2023**, *in review*.

7. Coradini, M.; Scoon, G.; Lebreton, J.-P. Venus Sample Return: Assessment Study Report. *Venus sample return Assess. study report/M. Coradini* **1998**.

8. Sweetser, T.; Cameron, J.; Chen, G.-S.; Cutts, J.; Gershman, B.; Gilmore, M.; Hall, J.; Kerzhanovich, V.; McRonald, A.; Nilsen, E. Venus Surface Sample Return: A Weighty High-Pressure Challenge. **1999**.

9. Sweetser, T.; Peterson, C.; Nilsen, E.; Gershman, B. Venus Sample Return Missions—a Range of Science, a Range of Costs. *Acta Astronaut.* **2003**, *52* (2–6), 165–172.

10. Rodgers, D.; Gilmore, M.; Sweetser, T.; Cameron, J.; Chen, G.-S.; Cutts, J.; Gershman, R.; Hall, J. L.; Kerzhanovich, V.; McRonald, A.; Nilsen, E.; Petrick, W.; Sauer, C.; Wilcox, B.; Yavrouian, A.; Zimmerman, W. *Venus Sample Return. A Hot Topic*; 2000; Vol. 7. https://doi.org/10.1109/AERO.2000.879315.

11. Shibata, E.; Lu, Y.; Pradeepkumar, A.; Cutts, J. A.; Saikia, S. J. A Venus Atmosphere Sample Return Mission Concept: Feasibility and Technology Requirements. In *Planetary Science Vision 2050 Workshop*; 2017; Vol. 1989, p 8164.

12. Ajluni, T.; Everett, D.; Linn, T.; Mink, R.; Willcockson, W.; Wood, J. OSIRIS-REx, Returning the Asteroid Sample. In *2015 IEEE Aerospace Conference*; IEEE, 2015; pp 1–15.

13. Wiens, R. C.; Reisenfeld, D.; Jurewicz, A.; Burnett, D. The Genesis Solar-Wind Mission: First Deep-Space Robotic Mission to Return to Earth. In *Sample Return Missions*; Elsevier, 2021; pp 105–122.

14. Brownlee, D. E.; Tsou, P.; Anderson, J. D.; Hanner, M. S.; Newburn, R. L.; Sekanina, Z.; Clark,

B. C.; Hörz, F.; Zolensky, M. E.; Kissel, J. Stardust: Comet and Interstellar Dust Sample Return Mission. *J. Geophys. Res. Planets* **2003**, *108* (E10).

15. Brownlee, D. The Stardust Mission: Analyzing Samples from the Edge of the Solar System. *Annu. Rev. Earth Planet. Sci.* **2014**, *42*, 179–205.

16. Yoshikawa, M.; Kawaguchi, J.; Fujiwara, A.; Tsuchiyama, A. Hayabusa Sample Return Mission. *Asteroids IV* **2015**, *1* (397–418), 1.

17. Watanabe, S.; Tsuda, Y.; Yoshikawa, M.; Tanaka, S.; Saiki, T.; Nakazawa, S. Hayabusa2 Mission Overview. *Space Sci. Rev.* **2017**, *208* (1), 3–16.

18. Xiao, L.; Qian, Y.; Wang, Q.; Wang, Q. The Chang'e-5 Mission. In *Sample Return Missions*; Elsevier, 2021; pp 195–206.

19. Knollenberg, R. G.; Hunten, D. M. The Microphysics of the Clouds of Venus: Results of the Pioneer Venus Particle Size Spectrometer Experiment. *J. Geophys. Res. Sp. Phys.* **1980**, *85* (A13), 8039–8058. https://doi.org/10.1029/JA085IA13P08039.

20. Knollenberg, R. G.; Hunten, D. M. Clouds of Venus: Particle Size Distribution Measurements. *Science (80-.).* **1979**, *203* (4382), 792–795.

21. King, R.; Bywaters, K.; Zacny, K.; Seager, S.; Petkowski, J. Tape and Roller Sampling System for Flexible Venusian Atmosphere Aerosol Capture and Delivery. I.

22. Brinckerhoff, W. B.; Ten Kate, I. L.; Hernstig, T.; Mellerowicz, B.; Wilson, J.; Zacny, K.; Mumm, E.; Romani, E. J.; Conrad, P.; Franz, H. B.; Mahaffy, P. R.; Corrigan, C. M.; Onstott, T. C. Precision Subsampling System for Mars and Beyond. *Proc. 12th Int. Conf. Eng. Sci. Constr. Oper. Challenging Environ. - Earth Sp. 2010* **2010**, 1364–1381. https://doi.org/10.1061/41096(366)123.

23. Moeller, R. C.; Jandura, L.; Rosette, K.; Robinson, M.; Samuels, J.; Silverman, M.; Brown, K.; Duffy, E.; Yazzie, A.; Jens, E.; Brockie, I.; White, L.; Goreva, Y.; Zorn, T.; Okon, A.; Lin, J.; Frost, M.; Collins, C.; Williams, J. B.; Steltzner, A.; Chen, F.; Biesiadecki, J. The Sampling and Caching Subsystem (SCS) for the Scientific Exploration of Jezero Crater by the Mars 2020 Perseverance Rover. *Space Sci. Rev.* **2021**, *217* (1), 1–43. https://doi.org/10.1007/S11214-020-00783-7/FIGURES/49.

24. Knollenberg, R. G.; Hunten, D. M. The Microphysics of the Clouds of Venus: Results of the Pioneer Venus Particle Size Spectrometer Experiment. *J. Geophys. Res. Sp. Phys.* **1980**, *85* (A13), 8039–8058.

25. Knollenberg, R. G. A Reexamination of the Evidence for Large, Solid Particles in the Clouds of Venus. *Icarus* **1984**, *57* (2), 161–183.

26. Forest, I.-S. *The Corrosion Resistance of Nickel-Containing Alloys in Sulfuric Acid and Related Compounds*; 1983.

27. Patterson, M. A.; Rao, A. V. GPOPS − II: A MATLAB Software for Solving Multiple-Phase Optimal Control Problems Using Hp-Adaptive Gaussian Quadrature Collocation Methods and Sparse Nonlinear Programming. *ACM Trans. Math. Softw* **2014**, *41* (1). https://doi.org/10.1145/2558904.

28. Sutton, G. P.; Biblarz, O. *Rocket Propulsion Elements*, 7th ed.; 2001.

29. Schiffer, R. A.; Beck, A. J. *Models of Venus Atmosphere*; 1968.

30. Cheung, K.; Jun, W.; Lee, C.; Lightsey, G. Single-Satellite Real-Time Positioning of Balloon and Helicopiter for Aerial Exploration in Extra-Terrestrial Atmosphere. In *70th International Aeronautical Congress*; IAF, 2019.

31. Yang, B.; He, F.; Jin, J.; Xiong, H.; Xu, G. DOA Estimation for Attitude Determination on Communication Satellites. *Chinese J. Aeronaut.* **2014**, *27* (3), 670–677. https://doi.org/10.1016/J.CJA.2014.04.010.

32. Border, J. S.; Lanyi, G. E.; Shin, D. K. *Radiometric Tracking for Deep Space Navigation*; Advances in the Astronautical Sciences: San Diego, 2008.

33. Preton, R.; Sagdeev, R. Z.; Blamont, J.; Matveenko, L. I.; Linkin, V. M.; Kerzhanovich, V. V.; Severnyj, A. B.; Laurans, G.; Hildebrand, C.; Purcell, G.; Finley, S.; Stelzried, C.; Ellis, J.; Petit, G.; Boloh, L.; Ortega-Molina, A.; Rosolen, L.; Boichat, A.; Biraud, F.; Collin, D.; Preton, R.; Sagdeev, R. Z.; Blamont, J.; Matveenko, L. I.; Linkin, V. M.; Kerzhanovich, V. V.; Severnyj, A. B.; Laurans, G.; Hildebrand, C.; Purcell, G.; Finley, S.; Stelzried, C.; Ellis, J.; Petit, G.; Boloh, L.; Ortega-Molina, A.; Rosolen, L.; Boichat, A.; Biraud, F.; Collin, D. The VEGA Balloon Experiment - Initial Results from the Global Radio Tracking. *Sov. Astron. Lett.* **1986**, *12*, 25–29.

34. Frazier, W.; McElrath, T.; Lee, C. Navigation and Communicatoin through the Venusian Clouds Design Concept Summary. In *2022 AAS/AIAA Astrodynamics Specialist Conference*; 2022.

35. Gustafson, E. D.; Martin-Mur, T.; Kruizinga, G.; Seubert, J. Mars 2020 Radiometric Data and Telemetry Processing, Attitude Estimation, and Thruster Calibration for Orbit Determination. In *2021 AAS/AIAA Astrodynamics Specialist Conference*; AAS, 2021.

36. Gustafson, E. D.; Kruizinga, G. L.; Martin-Mur, T. J.; Kruizinga, G. L.; Martin-Mur, T. J. Mars Science Laboratory Orbit Determination Data Pre-Processing. In *2013 AAS/AIAA Spaceflight Mechanics Meeting*; AAS, 2013.

37. Mohammadi, S.; Ghani, A.; Sedighy, S. H. Direction-of-Arrival Estimation in Conformal Microstrip Patch Array Antenna. *IEEE Trans. Antennas Propag.* **2018**, *66* (1), 511–515. https://doi.org/10.1109/TAP.2017.2772085.

38. Sánchez-Lavega, A.; Lebonnois, · Sebastien; Imamura, · Takeshi; Read, · Peter; David Luz, ·; Bézard, B.; Russell, C. T.; Satoh, T.; Smrekar, S. E.; Wilson, C. F.; Sánchez-Lavega, B. A. The Atmospheric Dynamics of Venus. *Sp. Sci. Rev. 2017 2123* **2017**, *212* (3), 1541–1616. https://doi.org/10.1007/S11214-017-0389-X.

39. Sagdeev, R. Z.; Linkin, V. M.; Blamont, J. E.; Preston, R. A. The VEGA Venus Balloon Experiment. *Science (80-.).* **1986**, *231* (4744), 1407–1408.

40. Kremnev, R. S.; Linkin, V. M.; Lipatov, A. N.; Pichkadze, K. M.; Shurupov, A. A.; Terterashvili, A. V; Bakitko, R. V; Blamont, J. E.; Malique, C.; Ragent, B. VEGA Balloon System and Instrumentation. *Science (80-.).* **1986**, *231* (4744), 1408–1411.

41. Sagdeev, R. Z.; Linkin, V. M.; Kerzhanovich, V. V; Lipatov, A. N.; Shurupov, A. A.; Blamont, J. E.; Crisp, D.; Ingersoll, A. P.; Elson, L. S.; Preston, R. A. Overview of VEGA Venus Balloon in Situ Meteorological Measurements. *Science (80-.).* **1986**, *231* (4744), 1411–1414.

42. Buchanan, W. P. Aerial Platform Design Options for a Life-Finding Mission at Venus and the Development of a Singularity-Free Dynamical Model for a Notional Venus Life Finder Sample Return Vehicle Using Euler Parameters, Purdue University, 2022.